R[illegible]3-88

RESEARCH ON THE ELECTROSTATIC GENERATION AND ACCELERATION OF SUBMICRON-SIZE PARTICLES

J. COHEN

SPACE TECHNOLOGY LABORATORIES, INC.
REDONDO BEACH, CALIFORNIA

MAY 1963

AERONAUTICAL RESEARCH LABORATORIES
OFFICE OF AEROSPACE RESEARCH
UNITED STATES AIR FORCE

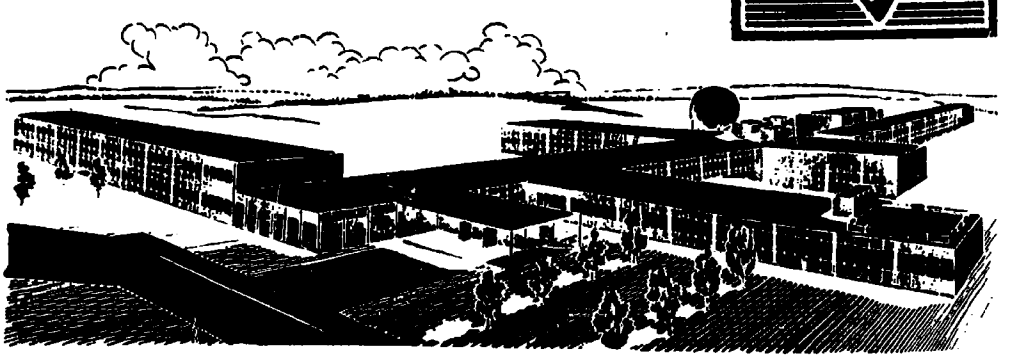

NOTICES

When Government drawings, specifications, or other data are used for any purpose other than in connection with a definitely related Government procurement operation, the United States Government thereby incurs no responsibility nor any obligation whatsoever; and the fact that the Government may have formulated, furnished, or in any way supplied the said drawings, specifications, or other data, is not to be regarded by implication or otherwise as in any manner licensing the holder or any other person or corporation, or conveying any rights or permission to manufacture, use, or sell any patented invention that may in any way be related thereto.

- - - - - - - - -

Qualified requesters may obtain copies of this report from the Armed Services Technical Information Agency, (ASTIA), Arlington Hall Station, Arlington 12, Virginia.

- - - - - - - - -

This report has been released to the Office of Technical Services, U. S. Department of Commerce, Washington 25, D. C. for sale to the general public.

- - - - - - - - -

Copies of ARL Technical Documentary Reports should not be returned to Aeronautical Research Laboratory unless return is required by security considerations. contractual obligations, or notices on a specific document.

1 - 10 - 300 - 161 - 8/29/63

Aeronautical Research Laboratories, Wright-Patterson AFB, O. RESEARCH ON THE GENERATION AND ACCELERATION OF SUBMICRON-SIZE PARTICLES by E. Cohen, Space Technology Labs., Inc., Redondo, Beach Calif. May 1963. 87 p. incl. illus. (Project 7116;Task 7116-03) (Contract AF 33(616)-6775) (ARL 63-88) Unclassified Report

The research involved in generating submicron-size positively charged liquid droplets is described. The droplets formed may be either liquid-metal, or organic fluids. An analysis is developed to indicate the relation-

(over)

UNCLASSIFIED

ship between particle size and the parameters of field emission and surface tension. Charge/mass ratios were obtained using either a single particle detector or one of two quadrupole focussing mass spectrometers. Charge/mass distributions are shown for both metals and organic fluids.

UNCLASSIFIED

Aeronautical Research Laboratories, Wright-Patterson AFB, O. RESEARCH ON THE GENERATION AND ACCELERATION OF SUBMICRON-SIZE PARTICLES by E. Cohen, Space Technology Labs., Inc., Redondo, Beach Calif. May 1963. 87 p. incl. illus. (Project 7116;Task 7116-03) (Contract AF 33(616)-6775) (ARL 63-88) Unclassified Report

The research involved in generating submicron-size positively charged liquid droplets is described. The droplets formed may be either liquid-metal, or organic fluids. An analysis is developed to indicate the relation-

(over)

UNCLASSIFIED

ship between particle size and the parameters of field emission and surface tension. Charge/mass ratios were obtained using either a single particle detector or one of two quadrupole focussing mass spectrometers. Charge/mass distributions are shown for both metals and organic fluids.

UNCLASSIFIED

ARL-63-88

RESEARCH ON THE ELETROSTATIC GENERATION AND ACCELERATION OF SUBMICRON-SIZE PARTICLES

E. COHEN

SPACE TECHNOLOGY LABORATORIES, INC.
REDONDO BEACH, CALIFORNIA

MAY 1963

CONTRACT AF 33 (616)-6775
PROJECT 7116
TASK 7116-03

FOREWORD

The document, "Research on the Electrostatic Generation and Acceleration of Submicron-size Particles," is a final report. The Physical Electronics Laboratory, Physical Research Division, Space Technology Laboratories, Inc., One Space Park, Redondo Beach, California is responsible for the research reported and for the preparation of the technical report.

The work was performed under Contract AF33(616)-6775, Project 7116, "Energy Conversion Research," Task 7116-03, "New Energy Conversion Techniques." The period reported upon extended from August 1959 to April 1963. During this period our experimental investigation was undertaken to generate charged liquid droplets. The droplets were found to have charge/mass ratios extending from 200 coulombs/kilogram up to 755 coulombs/kilogram.

This final report has been made possible by the enthusiastic support and substantial contributions of many workers. They include E.C. Ashwell, A.H. Cho, E. Cohen, C.D. Hendricks, V.E. Krohn, D.B. Langmuir, N.L. Roy, H. Shelton, C. Somol, and G.C.K. Yeh at this laboratory as well as C.D. Hendricks, A.H. Cho, J.J. Hogan and J.M. Schneider at the University of Illinois and R.D. Sloan of Sloan Research Industries who prepared the electron micrograph.

We are greatly indebted to the sponsor, Aeronautical Research Laboratories, Office of Aerospace Research, and in particular, to E.D. Stephens for guidance and support of this program.

ABSTRACT

The research involved in generating submicron-size positively charged liquid droplets is described. The droplets formed may be either liquid metal, or organic fluids. An analysis is developed to indicate the relationship between particle size and the parameters of field emission and surface tension. Charge/mass ratios were obtained using either a single particle detector or one of two quadrupole focussing mass spectrometers. Charge/mass distributions are shown for both metals and organic fluids. Although ions were often found, particularly with the metal fluids, narrow peak distributions of charge/mass could be obtained with no appreciable number of ions when using the organic liquids. Photomicrographs of the operating point source and discrete jet spray patterns are illustrated. The effect upon the charge/mass peak to the mass flow rate and the potential of the point emitter is demonstrated. The efficiency of an ion engine as a function of charge/mass distribution about a peak has been evaluated for several typical curves. An analysis involving space charge limitations and the mechanism of droplet formation is discussed.

TABLE OF CONTENTS

		Page
I.	Introduction	1
II.	Source System	1
	A. Basic Components and Operation	1
	B. Materials	3
	C. Source Geometry	4
	D. Variables	5
III.	Detectors	5
	A. Single Particle Detector	5
	B. Massenfilter	10
	C. Photography	19
	D. Electron Microscopy	19
	E. Magnetic Deflection	19
IV.	Theoretical Considerations	20
	A. Fundamental Limits of Droplet Charge	20
	1. Ion Limit	20
	2. Rayleigh Limit	21
	3. Combination of Ion and Rayleigh Limits	23
	B. Shape of the Liquid at the End of the Source Tube	26
V.	Experimental Results	27
	A. Liquid Metals	27
	1. General	27
	2. Single Droplet Studies	28

TABLE OF CONTENTS (Cont.)

Page

3. Magnetic Deflection 32

4. Attempts to Eliminate Ions. 35

5. Massenfilter Studies of Ions. 36

6. Massenfilter Studies of Macroscopic Droplets. 39

7. Photomicrographs of Operating Source 42

8. Electron Microscopy 44

B. Fused Salts 44

C. Organic Liquids. 44

1. General 44

2. Single Droplet Studies. 46

3. Massenfilter Results. 48

4. Photomicrographs of Operating Source 68

VI. Discussion of Results 68

A. Summary. 68

References 77

Appendix A (Massenfilter). A-1

Appendix B (Analysis Involving Space Charge Limitation and Mechanism of Droplet Formation) B-1

LIST OF FIGURES

Figure		Page
1.	Source System with Single Particle Detector	2
2.	Source Tube with Ball at End	4
3.	Nickel Microsphere Sintering	6
4.	Glycerol Flow Rate (Sintered Tip)	7
5.	Single Particle Detector	8
6.	Massenfilter	11
7.	Schematic of Massenfilter	14
8.	Photograph of Massenfilter	15
9.	Resolution of Massenfilter	16
10.	Block Diagram of Massenfilter Electronics	17
11.	Circuit Diagram of Massenfilter Oscillator	18
12.	Specific Impulse vs. Radius	22
13.	Rayleigh Limit and Ion Limit	24
14.	Oscilliscope Traces from Single Metal Droplets at 6.8 kv Source Voltage	29
15.	Oscilliscope Traces from Single Metal Droplets at 6.0 kv Source Voltage	30
16.	Metal Droplet Charge as a Function of Pulse Length at 5.4 kv Source Voltage	33
17.	Metal Droplet Charge as a Function of Pulse Length at 6.0 kv Source Voltage	34
18.	Charge/Mass Distribution of Metal Droplets	40

LIST OF FIGURES (Cont.)

Figure		Page
19.	Photomicrographs of Source Operating with Woods Metal	43
20.	Electron Micrograph of Metal Droplets	45
21.	Charge/Mass Ratios and Radii of Individual Octoil Droplets	47
22.	Histogram of Octoil Droplet Radii	49
23.	Total Charge versus Charge-to-Mass Ratio for Glycerol Containing 3.5% Antimony Trichloride	51
24.	Total Mass vs. Charge/Mass Ratio of Glycerol Containing 3.5% Antimony Trichloride	53
25.	Total Charge vs. Charge/Mass Ratio of Glycerol Containing 7% Antimony Trichloride	54
26a.	Jet Pattern Sintered Nickel Tip	56
26b.	Jet Pattern Fiberfrax Tip	57
27.	Charge-to-Mass for Sintered Nickel Needle, Raw Data	65
28.	Mass Flow vs. Charge-to-Mass for Sintered Nickel Needle	66
29-35.	Photomicrographs of Source Operating with Octoil	69-75

Table		
1		59
2		60

RESEARCH ON THE GENERATION AND ACCELERATION OF SUBMICRON-SIZE PARTICLES

I. INTRODUCTION

This summary report covers the period extending from August 1959 to February 1963. It describes research on the generation of liquid droplets of submicron size. The type of source used for the generation of charged liquid droplets of various kinds is illustrated schematically in Figure 1. This source produces charged droplets from bulk liquid in a single step rather than attempting to generate and charge droplets or particles in separate operations. The study of this source has been pursued to the exclusion of other possible types because of the interesting fundamental effects which have been observed and because the charge-to-mass ratios on the droplets fall in a range which is of interest for possible electrostatic propulsion applications.

In the pages which follow, sections will be devoted to the source system, detectors developed and used to study the output of the source, theoretical considerations, the results of the various measurements, and a discussion of the results.

II. SOURCE SYSTEM

A. Basic Components and Operation

The essential elements of the original source system (Figure 1) are a reservoir of liquid, a source tube, a high vacuum region surrounding the source, a region of controlled pressure above the liquid reservoir, and a positive high voltage supply. The reservoir pressure and the high voltage control the flow of liquid through the source tube. With

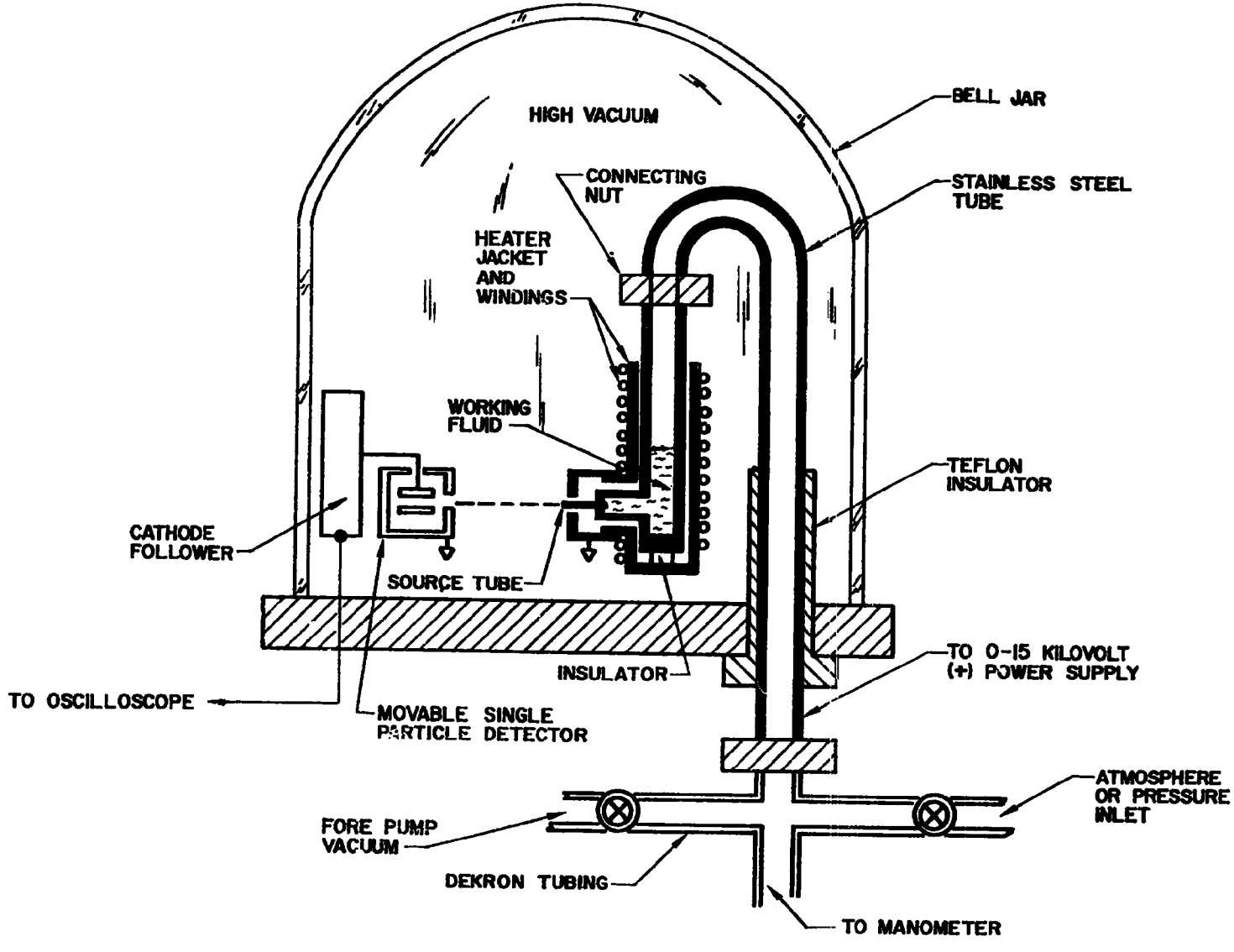

SOURCE SYSTEM WITH SINGLE PARTICLE DETECTOR

Figure 1. Source System with Single Particle Detector.

some materials (e.g., glycerol) the reservoir pressure required for the emission of charged droplets from the source is sufficient to cause the liquid to flow in the absence of the high voltage with no tip packing but when operating with other materials (e.g. eutectic mixtures of lead and bismuth) under conditions producing droplets of relatively high charge-to-mass ratio, the flow of liquid stops when the voltage is reduced by a few percent.

Positive, rather than negative, voltages are applied to the source tube as the latter would cause the field emission of electrons and limit the studies to low voltages and low charge-to-mass ratios which would be of very little interest.

A jacket may be positioned around the reservoir supporting heating coils which are used when elevated temperatures are desired. This jacket surrounds the source tube as well as the reservoir. The tube and reservoir are heated by radiation. The tube penetrates the jacket through a hole 0.25" in diameter. For a given applied voltage, the close proximity of the jacket, which is electrically grounded, increases the field at the tip of the source tube relative to the field which would exist if grounded surfaces were at a greater distance. However, the shape of the field at the end of the source tube is primarily determined by the shape of the end itself.

B. Materials

A variety of working fluids have been studied. It is convenient to classify them as organic liquids, organic liquids with dissolved ionic conductors, fused salts, and liquid metals.

The organic liquids investigated were silicone pump oil, octoil, and glycerol. The ionic conductors which were used as additives were antimony trichloride, urea mononitrate, tetra-n-butyl ammonium picrate, and hydroquinone. The only fused salt

considered was Draw-temp 275, a commercial mixture which probably contains nitrates and nitrites of sodium and potassium. The liquid metals studied were Wood's metals; tin; gallium; an eutectic mixture of lead and bismuth; and a mixture of lead, bismuth, and tin. Before use, glycerol-$SbCl_3$ solutions are processed by filtration through an 0.22 micron Millipore Filter and then dried by boiling off any water under reduced pressure.

C. Source Geometry

The size and shape of the source tube is of importance in determining the electric field and the rate of flow of working fluid at the end of the tube. Open, thin-walled tubes with inside diameters from 0.001" to 0.020" have been tried. Tubes from 0.005" to 0.020" have been packed at their emitting ends with machinable ceramic plugs, with Fiberfrax, and with glass wool. Restrictions have been created by crimping tubes at a distance from the emitting ends. An arrangement with a round ball mounted at the end of a tube (Figure 2) was also used. The ball had a diameter of 0.013" and was on a 0.006" shaft which tapered to 0.002" at the ball. The shaft was held by friction in a source tube of 0.007" inside diameter and 0.001" wall thickness with 0.002" clearance between the ball and the end of the source tube.

Figure 2. Source Tube with Ball at End.

The initial stainless steel hollow source tubes have been replaced by nickel tubes in order to avoid the reaction between the stainless steel and antimony trichloride. In place of the Fiberfrax packing, 0.002 inch nickel microspheres are sintered in the emission end of the tube. This is accomplished under vacuum at a temperature of 1250°C held for 30 minutes. Figure 3 is a schematic drawing of the system used. In Figure 4 is a typical flow rate run on glycerol through a sintered tip nickel needle. An external pressure of 8 inches of Hg was employed.

D. Variables

The parameters which were adjusted in order to achieve operation of the source and to investigate the effect of the variations on source operation included the high voltage, the reservoir pressure, the temperature of the working fluid, and the pressure in the jar containing the source. Also, a special grid could be installed and biased to greatly reduce the bombardment of the source tube by secondary electrons. Use of a new vacuum system reduced the bombardment of the source tube to the point where the grid was unnecessary. In addition, the source could be operated at a reduced direct voltage plus an alternating voltage (either 2 or 30 megacycles) which had positive peaks somewhat above the direct voltage needed to operate the source in the absence of the alternating voltage.

III. DETECTORS

A. Single Particle Detector

Considerable information has been obtained by studying the charge induced on small electrodes by individual charged droplets. A detector of this type is shown in Figure 5. Most of the work was done with a detecting electrode which was a

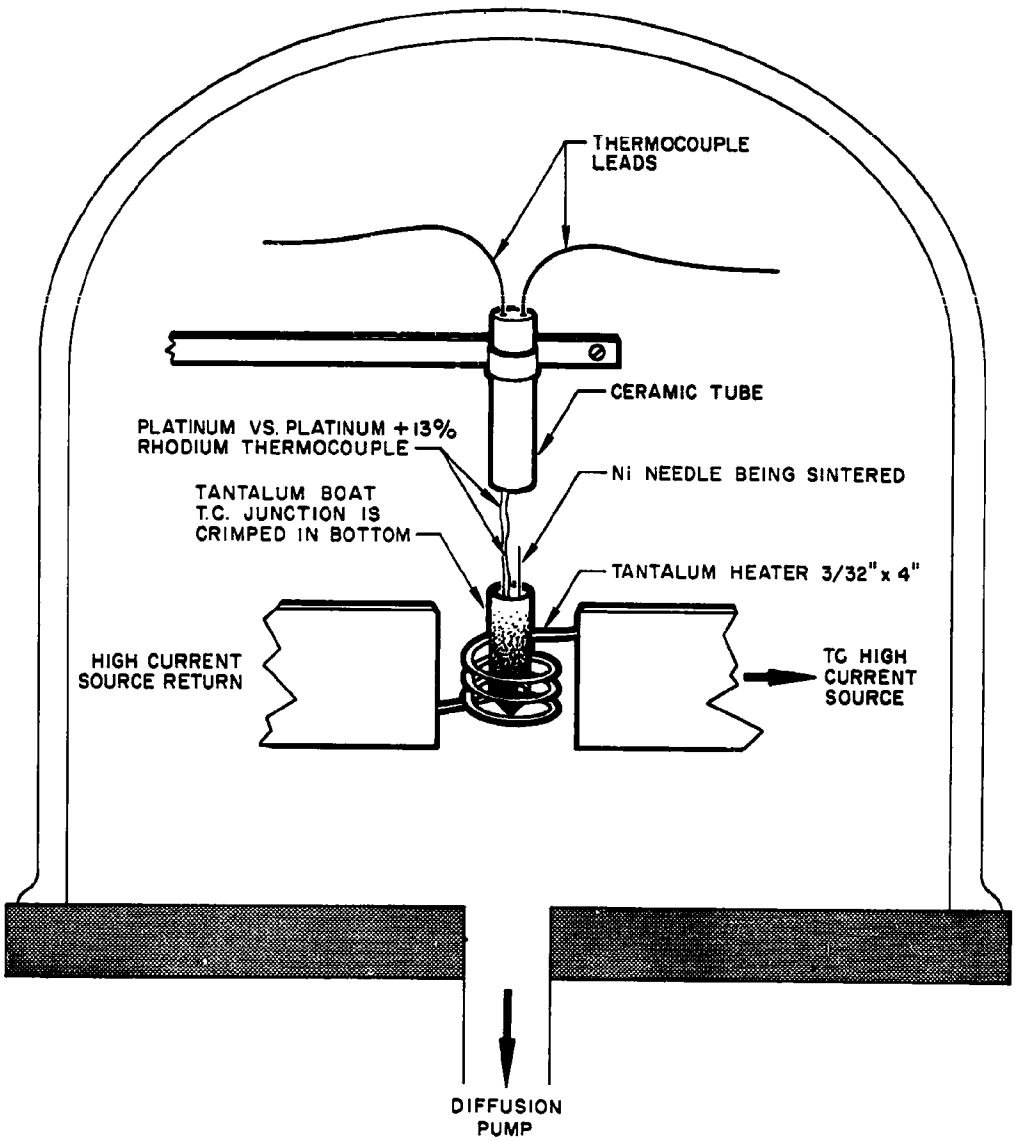

Figure 3. Nickel Microphere Sintering.

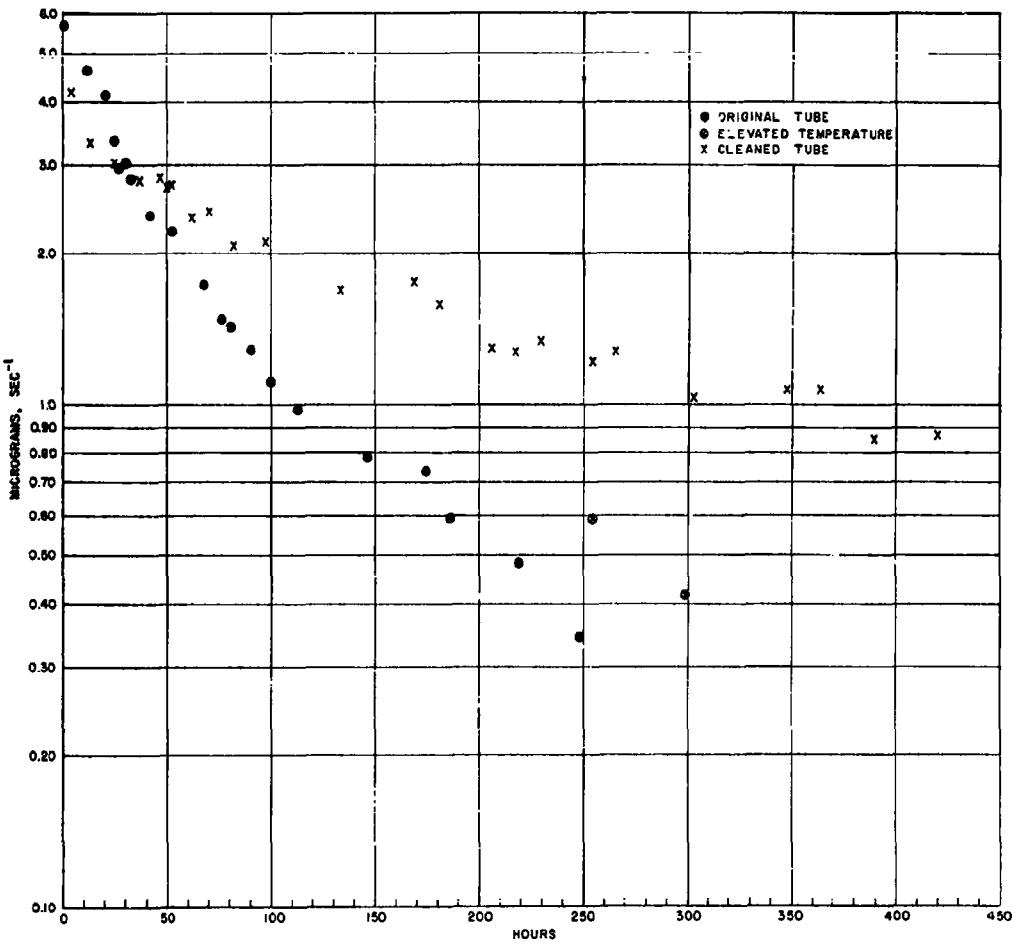

Figure 4. Glycerol Flow Rate (Sintered Tip)

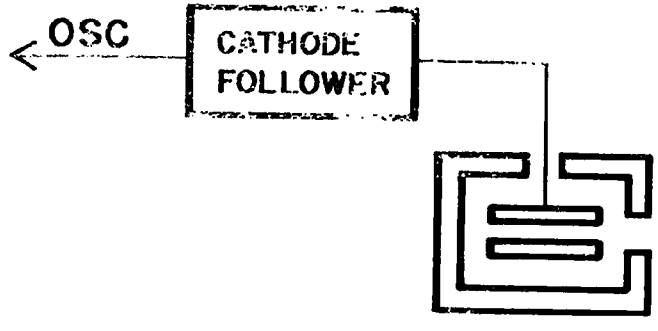

$$1.\quad \frac{Q}{M} = \frac{d^2}{2Vt^2}$$

$$2.\quad Q = \frac{CV_o}{G}$$

$$3.\quad M = \frac{2Vt^2 CV_o}{d^2 G}$$

$$4.\quad r = \left(\frac{3Vt^2 CV_o}{2\pi\rho d^2 G}\right)^{1/3}$$

Figure 5. Single Particle Detector.

cylinder 0.275" long and 0.020" in inside diameter. The droplets produced approximately rectangular pulses as they passed through the cylinder. These pulses were processed by a cathode follower circuit within the bell jar and displayed on an adjacent oscilloscope. Photographs of oscilloscope traces were taken when quantitative data were desired.

The height of a pulse is proportional to the charge of the detected droplet and the length is proportional to the droplet velocity v. Since the density of the droplet ρ, the accelerating (i.e., source) voltage V, the input capacity C of the cathode follower circuit with the detector attached, and the gain G of the electronic circuitry are readily available, one can calculate the velocity, charge-to-mass ratio Q/M, the charge Q, the mass M, and the radius r of a droplet with the following equations:

$$(1) \quad \frac{Q}{M} = \frac{d^2}{2Vt^2}$$

$$(2) \quad Q = \frac{CV_o}{G}$$

$$(3) \quad M = \frac{2Vt^2CV_o}{d^2G}$$

$$(4) \quad r = \left(\frac{3Vt^2CV_o}{2\pi\rho d^2G}\right)^{1/3}$$

where d is the length of the detecting cylinder, t the pulse length, and V_o the voltage of the pulse out of the electronic circuits.

Arrangements were made to rotate the single particle detector while the source was operating so that angular distributions could be studied.

The smallest charge detected on a droplet (above background noise) was 4.5×10^{-16} coulombs, about 3000 electron charges. While this limit could probably be extended somewhat, it was more convenient to use the detector described in the next section to investigate droplets with less charge.

B. Massenfilter

The Massenfilter transmits a range of charge-to-mass ratios which are stable in a time-dependent electric quadrupole field. Instruments of this type were first used by Paul[1] and his collaborators as mass separators and as spectrometers. This device is particularly suitable for studying droplets with charge-to-mass ratios many orders of magnitude less than atomic ions as very large regions of high magnetic field would be needed to investigate such droplets with conventional magnetic deflection techniques. A sketch of the original spectrometer used for the present investigations is shown in Figure 6. The electrodes of the spectrometer and the connecting cables form part of the tank circuit of the oscillator. Twelve frequency bands extending from 8 kc to 25 mc were used. The direct voltage for the quadrupole electrodes is obtained by rectifying the alternating voltage and selecting the desired fraction from a resistive divider network. As this fraction determines the resolution of the instrument, the scheme selected gives a resolution which is (to first order) independent of frequency and alternating voltage and which can be readily varied.

We might review at this time some of the problems experienced in obtaining the data to be reported.

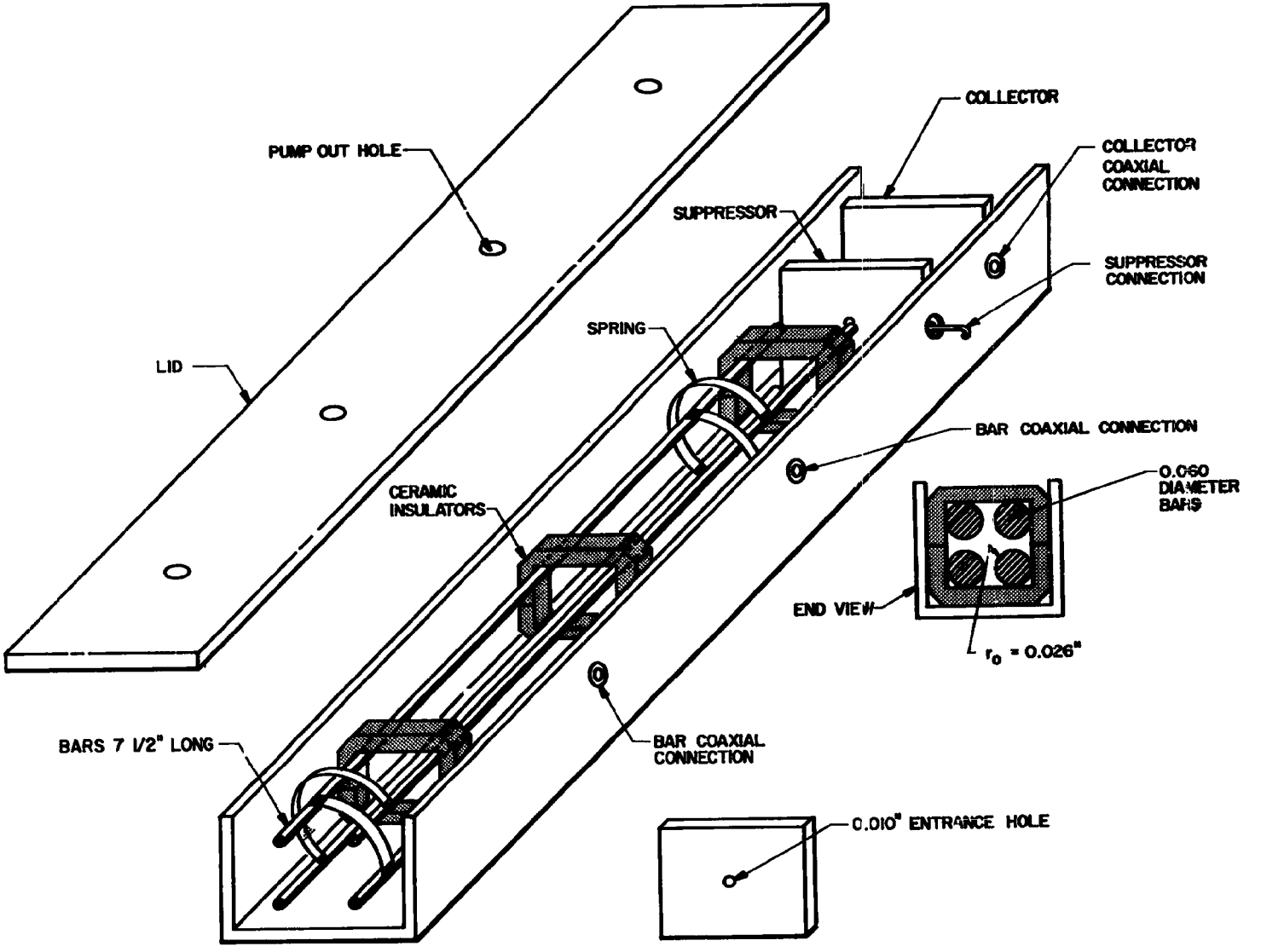
PUMP OUT HOLE
COLLECTOR
COLLECTOR COAXIAL CONNECTION
SUPPRESSOR
SUPPRESSOR CONNECTION
SPRING
LID
BAR COAXIAL CONNECTION
0.060 DIAMETER BARS
CERAMIC INSULATORS
END VIEW
r_0 = 0.026"
BARS 7 1/2" LONG
BAR COAXIAL CONNECTION
0.010" ENTRANCE HOLE
MASSENFILTER

Figure 6.

1) Our source tubes would plug up.
2) Arcing occurred and tubes would fuse.
3) Coupled with the arc was the relatively poor vacuum in the vicinity of the source tube, probably 5×10^{-4} mm Hg.
4) The stainless steel source tubes dissolved during metal studies (gallium and tin) and would also react with the antimony trichloride.
5) Tubes giving the most stable results were packed at the emission end with Fiberfrax. This material does not lend itself to obtaining the most consistent results.
6) The Massenfilter entrance aperture, 0.010 inches, would plug up with glycerol droplets.
7) It was difficult to orient the source tube to the Massenfilter.

All these problems appear to be soluble. The source liquid processing, discussed earlier, is filtered through an 0.22 micron Millipore Filter and then dried by boiling off the water under reduced pressure. By using a new vacuum system and inserting two nitrogen cold traps, one adjacent to the source assembly, we can reduce the pressure at the source of the droplets to 4×10^{-6} mm Hg. We have a working pressure with glycerol droplets of 5×10^{-5} mm Hg or better. The use of sintered nickel tubes has been described earlier.

We desired to keep the resolution of our Massenfilter constant but to enlarge the entrance aperture from 0.010 inches to 0.10 inches. This forced a redesign of our instrument. Along with the addition of two cold traps we have also made provisions to rotate the source tube about an axis perpendicular to the droplet beam and passing through the ejection end of the source tube. Unfortunately this one dimensional scan is not

sufficient to sample jets which do not lie in a horizontal plane. The parameters of the new Massenfilter follow:

1) Charge/Mass Range - 1 to 10^7 coulombs/kilogram
2) R.F. Voltage - 1000 volts peak, rail to ground
3) R.F. Frequency - 1000 cycles/sec. to 5 megacycles/sec.
4) D.C. Bias - 167.8 volts, adjustable to vary resolution
5) Field Radius - 0.827 cm.
6) Field Aperture - 0.10 inches
7) Rail Length - 45 inches

Measurements on the resolution of the Massenfilter, using a porous tungsten plug impregnated with potassium hydroxide as a source of ions, show that the two potassium isotope peaks at 39 and 41 can be easily resolved. The mass position of potassium 39 as determined from the Massenfilter, was correct to several percent.

Figure 7 is a schematic of the Massenfilter. Not shown is the ground plane surrounding the source tube. Figure 8 is a photograph of the instrument with quadrupoles exposed for test purposes. The resolution of the instrument is shown in Figure 9 with peaks for potassium 39 and 41. The block diagram and electronic circuit are pictured in Figures 10 and 11 respectively.

By varying the frequency and magnitude of the alternating voltage we are able to study charge-to-mass ratios from 1 to 10^7 coulombs per kilogram. The latter extreme corresponds to ions of atomic mass 10 and the former is more than four orders of magnitude below the highest ratio we have observed on macroscopic droplets. It is obvious that the huge range of charge-to-mass ratios which can be investigated with this spectrometer makes it a valuable instrument for the present studies. As

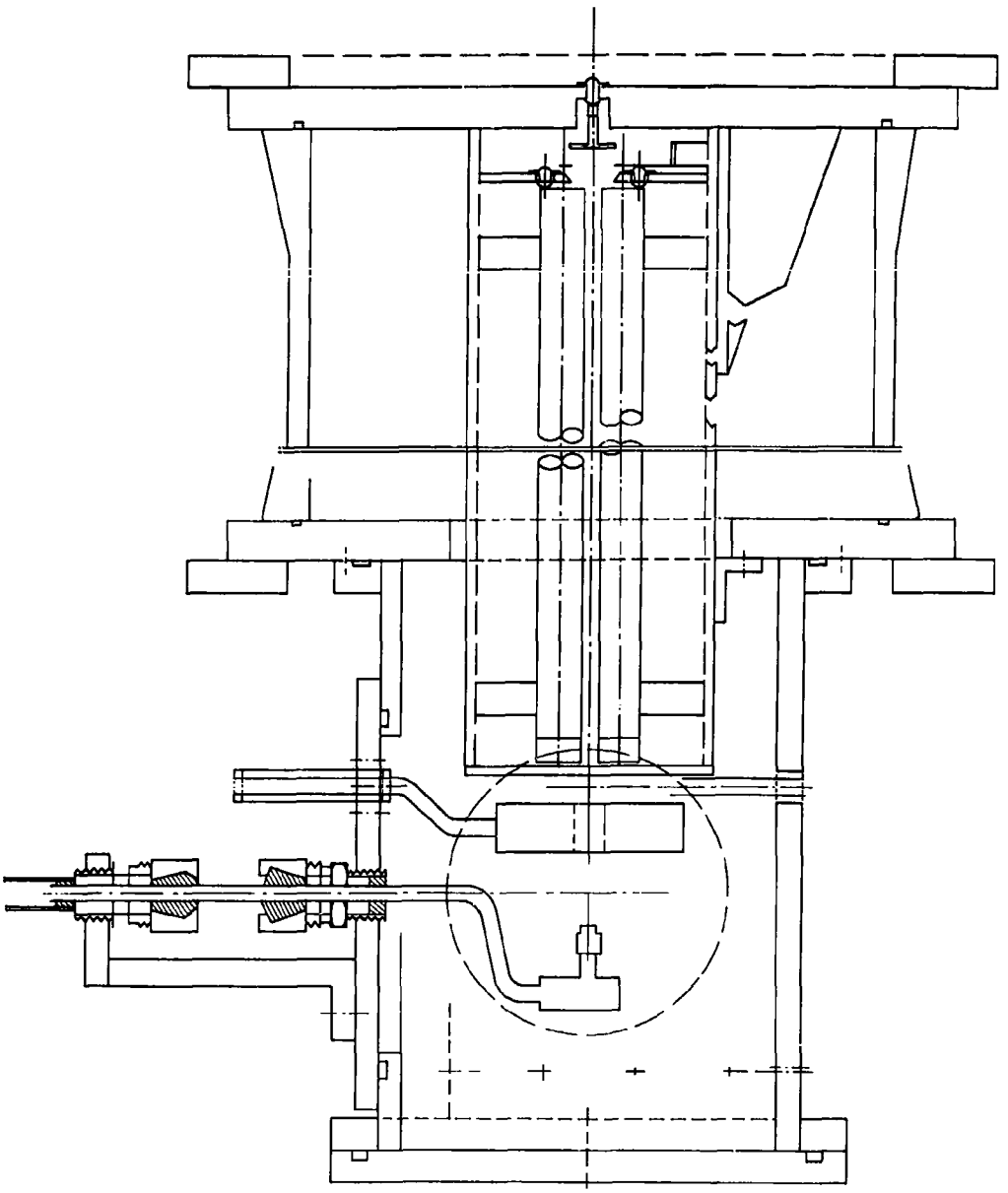

Figure 7. Schematic of Massenfilter.

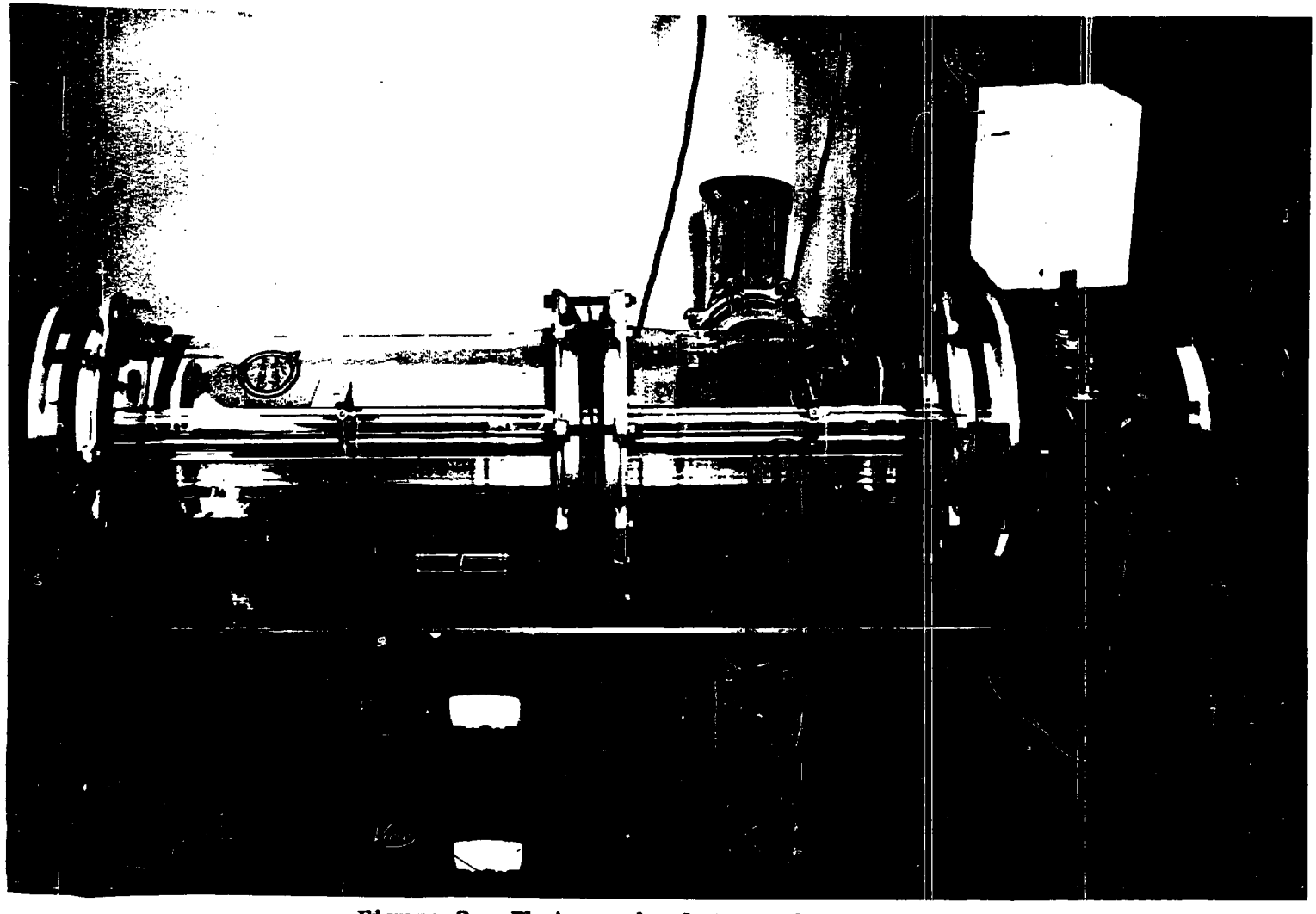

Figure 8. Photograph of Massenfilter

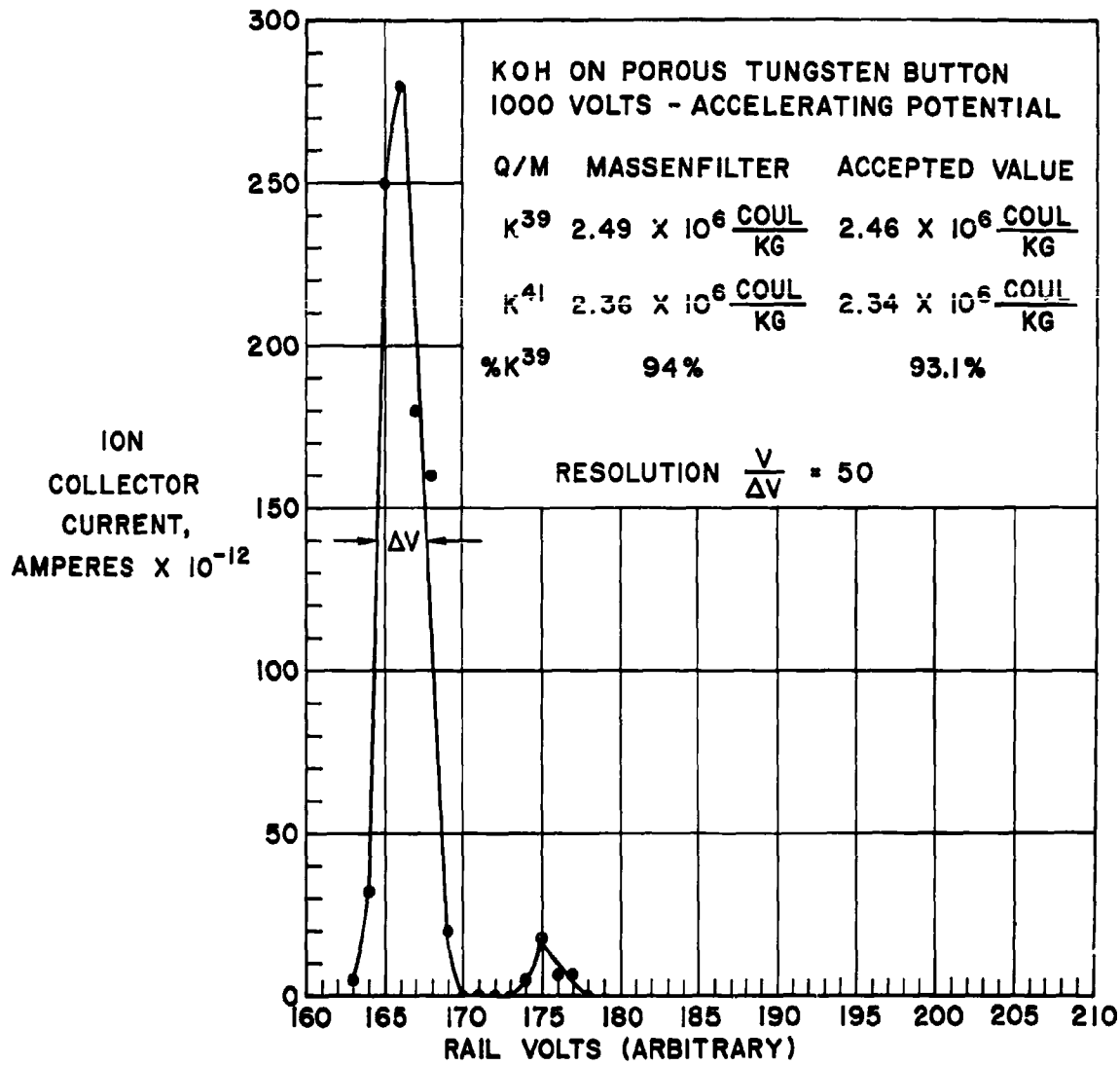

Figure 9. Resolution of Massenfilter.

MICROAMMETER (TOTAL CURRENT)
EXPERIMENT
MICROAMMETER (COLLECTOR)
H.V. SUPPLY 0–15KV DC AT 1 MA (FOR NEEDLE)
MASSEN FILTER
ELECTROMETER
FREQUENCY COUNTER
R.F. OSCILLATOR
B + SUPPLY 1500V AT 200 MA
FILAMENT SUPPLY 6.3V AT 5A

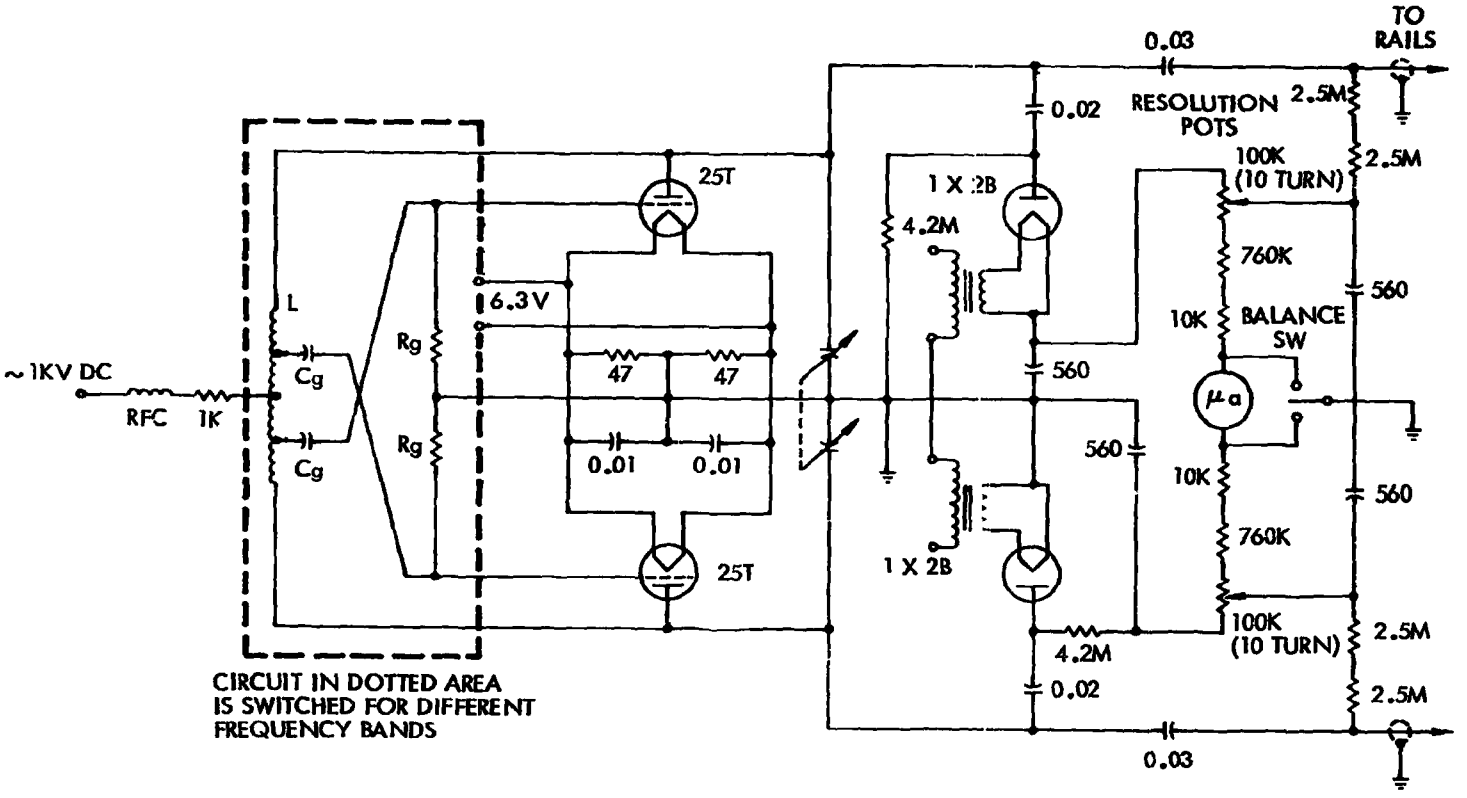

Figure 11. Circuit Diagram of Massenfilter Oscillator

this instrument measures total charge (transmitted current) as a function of charge-to-mass ratio, it does not permit a determination of individual droplet charge and mass. However, the data obtained with tho single particle detector in its less extensive range of usefullness are sufficient to supplement the Massenfilter data extensively. Appendix A discusses and develops the effect which ion accelerating potential has upon the Massenfilter resolution. In addition the finite bandwidth that the resulting resolution has upon the acceptance range is shown. An additional mode of operation, zero bias containment is described.

C. Photography

Part of the work under the present contract has been subcontracted with the University of Illinois where C. D. Hendricks and his collaborators have made extensive use of high speed photographic techniques to study the tip of the source tube and the emitted droplets. While individual droplets of submicron-size cannot be photographed, the pictures are of great value in that they show many interesting features of the shape assumed by the working fluid at the end of the source tube.

D. Electron Microscopy

Electron microscopy has been used to investigate the size distribution of metal droplets collected on microscope slides coated with parlodion films. As it is difficult to insure that a true sample of the droplets emitted by the source has been collected, this technique was not used extensively.

E. Magnetic Deflection

A set of aligned slits in a magnetic field was successfully used to separate ions and electrons from macroscopic charged droplets. This technique was abandoned in favor of the Massenfilter which is capable of providing more detailed

information about the spectrum of charge-to-mass ratios.

IV. THEORETICAL CONSIDERATIONS

A. Fundamental Limits of Droplet Charge

1. Ion Limit

One limitation on the amount of charge that can be carried by a solid particle or a liquid drop is that the electric field at the surface cannot exceed the field required to cause the emission of electrons in the case of negative charging or positive ions in the case of positive charging. Since the field emission of electrons occurs at much lower fields than the field emission of ions, the present program has employed positive charging exclusively in order to achieve high charge-to-mass ratios. Unfortunately, data concerning the field needed to cause the emission of ions from liquids are difficult to obtain. A rough estimate of 10^{10} volts/meter was used for liquid metals during the early stages of the present work. This was based on the fact that fields somewhat greater than this had been achieved by E. W. Muller[2] with solid tungsten. Subsequent data obtained under this program allowed us to infer that, for eutectic mixtures of lead and bismuth, this estimate was reasonably close, since an experimental value of approximately 10^{10} volts/meter was obtained from an indirect measurement for a number of droplets.

It is possible that substantially lower fields can cause the emission of ions from organic liquids.

For a spherical drop, the equation of the ion limit is

$$(5) \quad E = K$$

or $$(6) \quad Q = 4\pi\epsilon_o r^2 K$$

or $$(7) \quad \frac{Q}{M} = \frac{3\epsilon_o K}{\rho r}$$

where E is the electric field intensity at the surface of the drop and K is the minimum field which will cause the emission of ions from the liquid composing the drop. The proglem is shown graphically in Figure 12, which indicates the specific impulse obtainable as a function of particle radius for particles of various densities charged to different field strengths. An accelerating potential of 1 million volts is assumed.

2. Rayleigh Limit

An additional limitation which applies to liquid drops but not to solid particles was first calculated by Rayleigh[3]. This limit arises because a drop will break up into smaller drops if an attempt is made to charge it above the point where the outward pressure of the electric field at the surface of the drop exceeds the inward pressure of surface tension.

The equations of the Rayleigh limit are:

$$(8) \quad \frac{\epsilon_o E^2}{2} = \frac{2\gamma}{r}$$

or $$(9) \quad Q = 8\pi \sqrt{\gamma\epsilon_o}\, r^{1.5}$$

or $$(10) \quad \frac{Q}{M} = \frac{6\sqrt{\gamma\epsilon_o}}{\rho r^{1.5}}$$

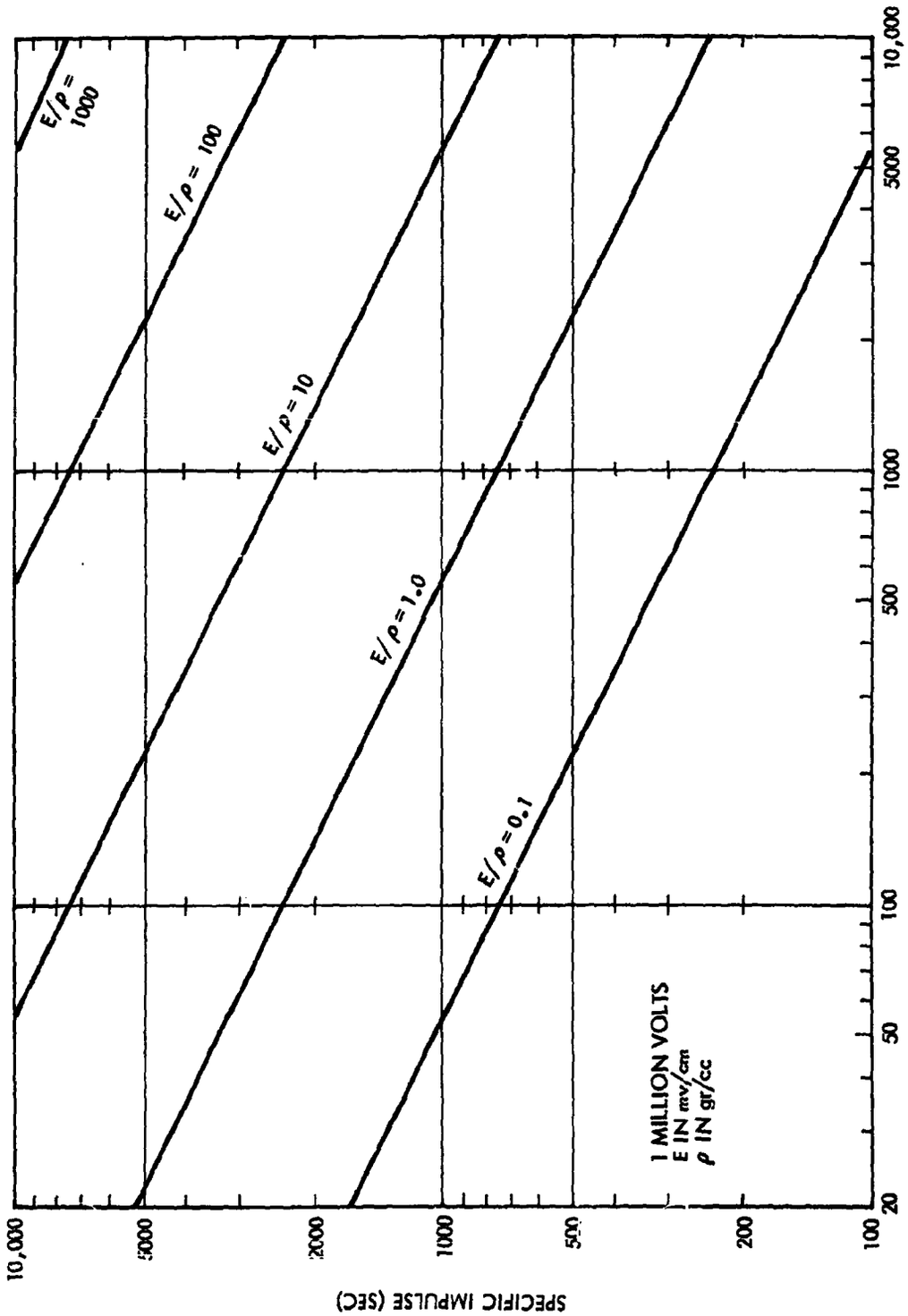

Figure 12. Specific Impulse vs. Radius.

where γ is the surface tension of the liquid forming the drop.

3. Combination of Ion and Rayleigh Limits

The radial dependence of the two limits is such that the Rayleigh limit will be the controlling restriction on the charge of large drops while the ion limit will predominate for small droplets. The droplet radius at which the two limits have the same value depends on the field K needed to cause field emission and the surface tension γ. Figure 13 is a plot of the two limits with $K = 10^{10}$ volts/meter and $\gamma = 0.4$ newtons/meter. These values are believed to be typical for liquid metals. The figure shows that the two limits become equal at a droplet radius of 20 Å and that a liquid of specific gravity 10 could have a charge-to-mass ratio as high as 12,000 coulombs/kilogram at this radius.

It is difficult to see how a source of the type used in the present work could produce droplets of radius smaller than the radius at which the ion limit and the Rayleigh limit intersect. A filament drawn from the liquid at the end of the source tube could have the radius at its tip continuously reduced by the electric field which would increase (at constant applied voltage) with the decreasing radius. But, when the radius at the tip reached the radius at which the ion and Rayleigh limits are equal, the emission of ions would commence, the field could not continue to increase, and smaller radii would not be produced. We believe that the results we have obtained demonstrate thatthe process just described occurs with liquid metals. With organic liquids, we believe that the flow of charge in filaments of the liquid is

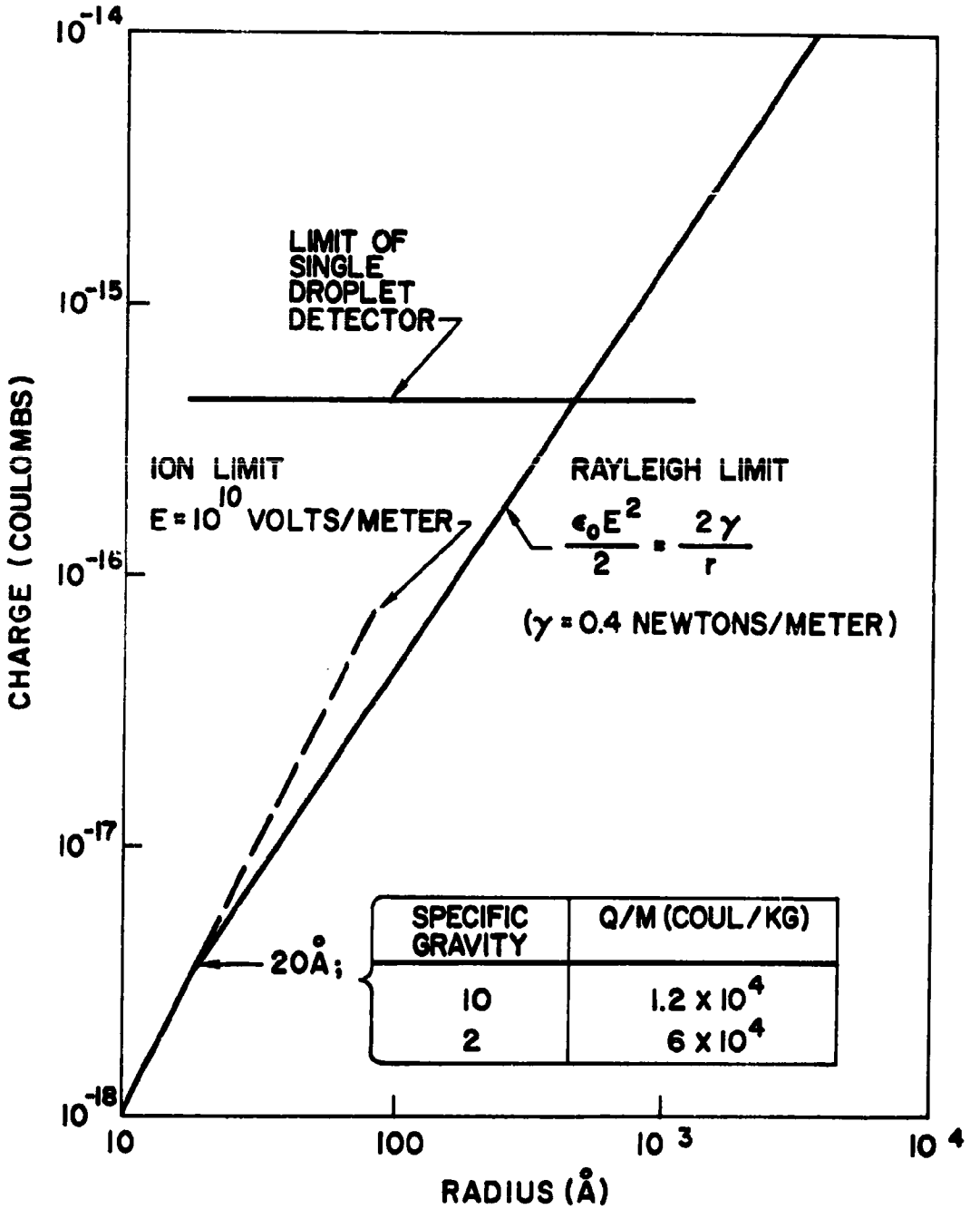

Figure 13. Rayleigh Limit and Ion Limit.

restricted to the extent that it is possible to operate the source without producing ions. The Ion-Rayleigh limit discussed here applies to a free spherical droplet. Of greater practical importance would be a model describing the behavior of the liquid in the vicinity of the source tube and in a space charge limiting field.

On the basis of present knowledge, a conceptual model of the liquid jet can be envisaged. It should be clear that much of this is still speculative. It is believed that the field operating upon the glycerol solution draws the liquid out and changes the shape of the more or less hemispherical drop which is present on the needle tip before the field is applied. The changed shape has the form of a long narrowing finger out of which the liquid flows. This finger contains net positive charge and is accelerated, the diameter narrowing as it moves outwards and speeds up. The current flow causes an IR drop which probably must be taken into consideration, especially at the smallest diameters. The break up of the jet into particles may occur in the manner characteristic of the break up of any jet of liquid under surface tension forces, except that the phenomena will be profoundly modified by the effect of the electric field. If the particles emerge at $q/m = 400$ coul/kg and with 5×10^{-7} amperes in a single jet, the particles will have a surface field strength 10^9 volts/m, a potential of 300 volts, a diameter of 700A and a mass of 2×10^{-19}kg. Each will contain approximately 500 electronic charges, presumable consisting of excess Sb^{+++} ions. This number of antimony ions amounts to about 1% of the total. These particles, 6×10^9 per second, will be

moving at 2.8 km/sec after dropping through the applied voltage (about 10 kv). The droplets would then be spaced about 10 diameters apart as they move toward the collector, 2×10^4 per linear cm. These characteristics are logically deduced in Appendix B.

The mechanism by which the thrust is exerted is an interesting subject for study. In a plain parallel configuration, the thrust is exerted on the accelerator electrode and there is net thrust because the space charge reduces the field at the emitter electrode. The case of the point emitter is treated in Appendix B. There it is shown that the current observed is that which would be predicted by space charge considerations. An interesting point is that this current is independent of the radius of the tip. This independence of tip size also infers that an array of needles whose emission merges and shields the needles from a single distant 10KV accelerator would also be space charge limited to about 1 microampere. Paralleling to 100 microamperes therefore requires separate 10KV accelerator apertures for each needle. Then the merging of the streams occur after passage through the apertures. From this point, acceleration and space charge effects can be treated conventionally.

B. Shape of the Liquid at the End of the Source Tube

Rayleigh's treatment[3] of the problem of the equilibrium of conducting masses charged with electricity involved calculation of the electrical energy and the energy associated with surface tension for a spherical droplet perturbed by small ripples which could be described by Legendre polynomials $P_n(\cos \theta)$. He then determined the stability or instability of the small perturbation.

By extending Rayleigh's treatment[4] we were able to show that the degree of instability is a maximum for a finite value of n. By assuming that the break up of the working fluid at the end of our source tube would be controlled by the mode (i.e., n value) which gave the greatest instability for disturbances of small amplitude and that the emitted droplets would have the radius of the nodes of the Legendre polynomial of this n value, we obtained reasonable agreement with the experimental results for octoil. However, for materials of higher conductivity the above assumptions are apparently not justified as no agreement was obtained with the experiments.

A proper theoretical treatment would involve spherical harmonics, $Y_{Lm}(\theta,\phi)$, constrained at the source tube and would attempt to follow the disturbance as its amplitude increased beyond the point where the Rayleigh assumption of small amplitude is valid.

V. EXPERIMENTAL RESULTS

A. Liquid Metals

1. General

The main difference in the results obtained with the various liquid metals is that gallium and tin dissolved the stainless steel source tubes so rapidly that it was difficult to obtain data, whereas the other metals did not attack the steel. All of the liquid metals investigated emitted large numbers of metallic ions along with metal droplets having a broad distribution of charge-to-mass ratios. When the end of a source tube was properly wetted by a liquid metal, it was possible to operate throughout a range of high voltages by adjusting the pressure in the reservoir. If the pressure was reduced while the source was operating, the emission

of ions and droplets could cease. Operation could then be restored by increasing the voltage. The total current tended to increase rapidly if the voltage was increased beyond the minimum needed to achieve source operation. In general, it was possible to use operating voltages from five to eight kilovolts with the liquid metals. Most of the work with liquid metals was done with open stainless steel source tubes of 0.005" inside diameter or with a ball at the end of a 0.007" source tube. However, other sizes of open tubes, tubes packed with wires, tubes constricted at a distance from their end, and glass tubes were also used.

The droplets and ions from liquid metals were emitted into a broad cone in front of the source tube. The tube and ball arrangement produced some interesting angular distributions which will be discussed, but the presence of discrete jets was never observed.

2. Single Droplet Studies

Wood's metal from a 0.005" open source tube was investigated with the single particle detector. Data obtained with other detectors indicate that similar results would be obtained if the other liquid metals were studied with this detector. Some examples of pulses produced by droplets of Wood's metal passing through the cylindrical detector described in Section III A are shown in Figure 14 and 15. In Figure 14, the oscilloscope traces were taken when the source was operating at 6.8 kv where all droplets produced pulses near or below the limit of detection. The sweep speed was 5 μsec/cm and the sensitivity 3.5×10^{-16} coulombs/cm. The largest pulse was from a droplet with a radius of

Figure 14. Oscilliscope Traces from Single Metal Droplets at 6.8 kv Source Voltage.

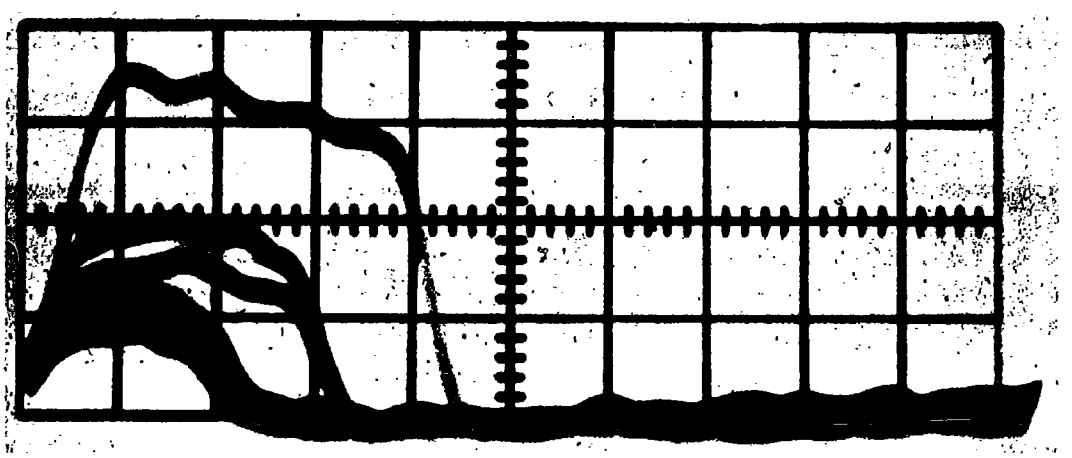

Figure 15. Oscilliscope Traces from Single Metal Droplets at 6.0 kv Source Voltage.

570 Å, a charge-to-mass ratio of 60 coulombs/kilogram, and an electric field of 13.8×10^8 volts/meter at its surface. The smaller pulses were not considered suitable for measurement of pulse length.

Figure 15 shows traces taken at a lower accelerating voltage, 6.0 kv. The sweep speed was 5 μsec/cm and the sensitivity 4.5×10^{-16} coulombs/cm. The high frequency response of the system had been reduced relative to the situation of Figure 6. The small, rounded pulses are from a group of droplets near the limit of detection. These droplets had a radius of 500 Å, a charge-to-mass ratio of 80 coulombs/kilogram, and a field of 1.6×10^9 volts/meter at their surface. The largest pulse in this figure was from a droplet with a radius of 1500 Å. It had a charge-to-mass ratio of 12 coulombs/kilogram and a field at its surface of 6.7×10^8 volts/meter.

In general, during the course of the investigation of Wood's metal with the single particle detector, the number of pulses was observed to increase rapidly with decreasing pulse height until one reached the limit of detection. This indicated that the peak of the curves representing number of particles or total charge versus radius, charge-to-mass ratio, or individual particle charge would all fall below the limit of detection and that the droplets at the peak of these distributions would have a smaller radius, a smaller charge, and a higher charge-to-mass ratio than any of the droplets producing detectable pulses. Since the peaks of these distributions could not be reached by the single particle detector, no attempt was made to obtain quantitative data on the distribution of pulses versus pulse height. Instead, data were taken in such a way that, for a given pulse height

(charge), the true distribution of pulse lengths (charge-to-mass ratios) would be detected. Figures 16 and 17 show some of the results obtained. For convenience, the raw data have been plotted with the position of the Rayleigh limit and some lines of constant droplet radius shown for reference.

The larger droplets of Figure 16 fall appreciably below the Rayleigh limit while the smaller droplets are somewhat closer to this limit. On the other hand, all of the droplets of Figure 17 fall rather close to the Rayleigh limit. In general, the droplets near the limit of detection (500 Å) were observed to be charged close to the Rayleigh limit whereas larger droplets sometimes fell below this limit by a factor of three or more.

It was observed that the charge of the droplets increased toward the Rayleigh limit and that the relative number of large droplets decreased when the source current was increased or when the reservoir pressure was decreased and the operating voltage increased.

The latter trend (with voltage and pressure) was so marked that we were unable to detect droplets with the single particle detector at operating voltages above about 7 kv although there was ample evidence that many droplets were being produced below the limit of detection of the single particle detector.

3. Magnetic Deflection

A magnetic field was used in conjunction with a pair of slits to separate ions from macroscopic droplets and the total current to a collector was measured. Arrangements were made to bias the collector so that the

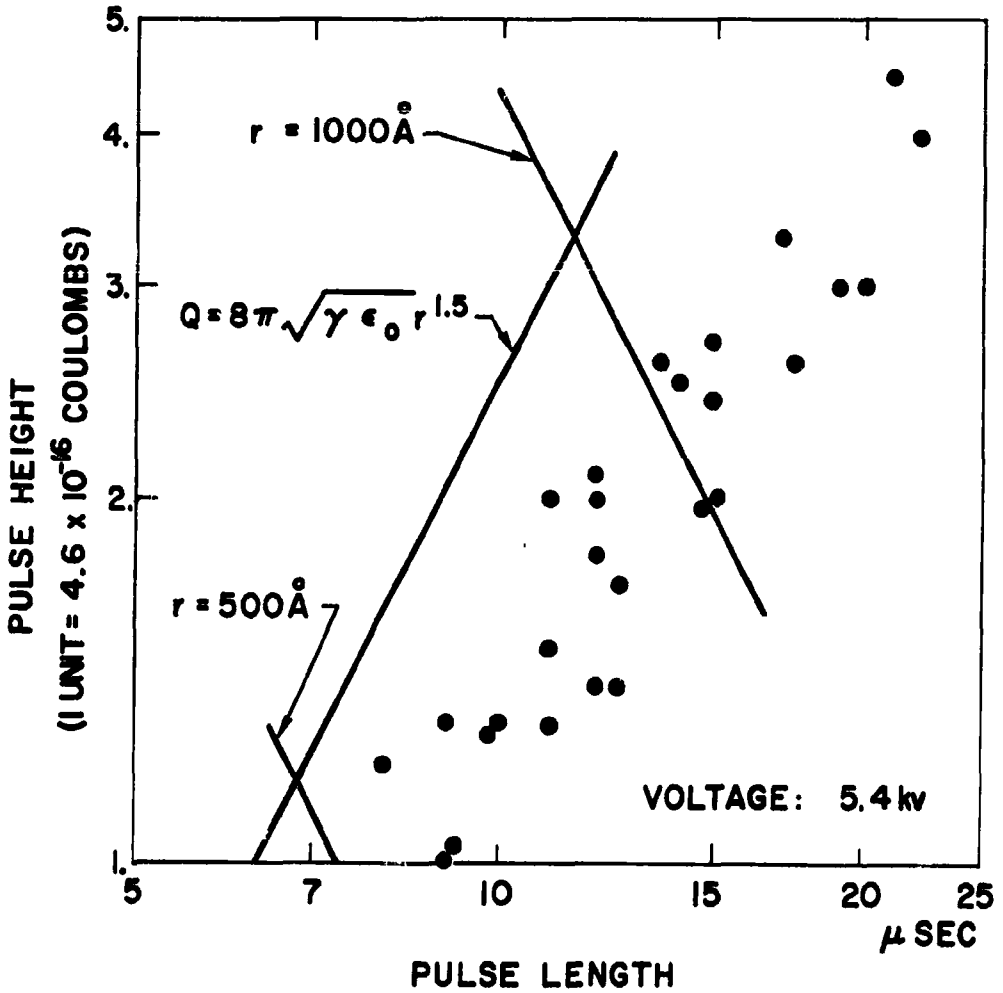

Figure 16. Metal Droplet Charge as a Function of Pulse Length at 5.4 kv Source Voltage.

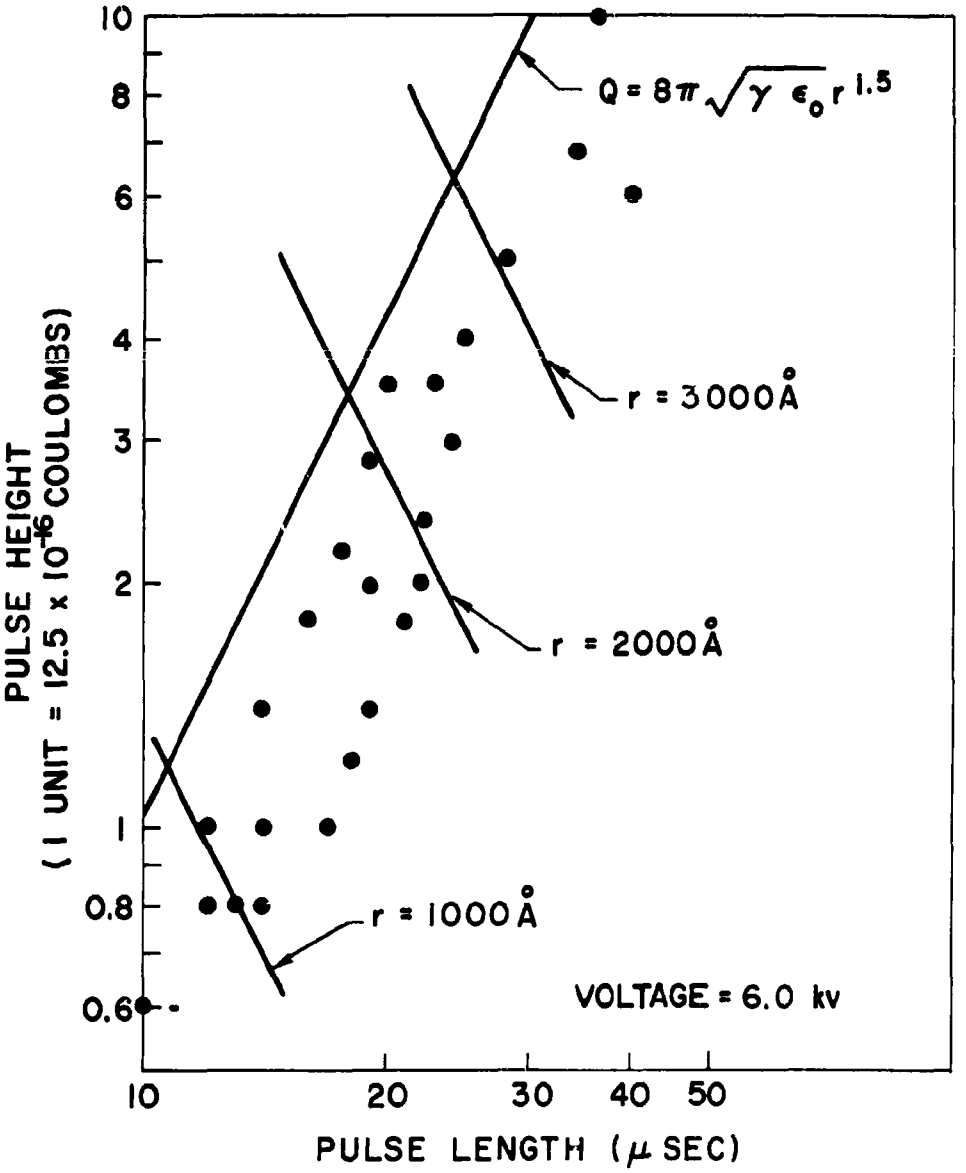

Figure 17. Metal Droplet Charge as a Function of Pulse Length at 6.0 kv Source Voltage.

contribution of secondary electrons to the total current could be determined. The measurements indicated that about two-thirds of the current was carried by ions, one third by electrons, and only about one percent by macroscopic droplets. The total droplet current was about one microampere.

4. Attempts to Eliminate Ions

A number of changes were tried in an attempt to operate the source so that a smaller number of ions would be produced along with the metal droplets. The magnetic deflection scheme was used to monitor the effect of the changes.

One possibility investigated was the substitution of an alloy of bismuth, lead, and tin for Wood's metal which is an alloy of these three elements plus cadmium. If the relatively high vapor pressure of cadmium had been essential for the production of large numbers of ions, the ion production should have been drastically reduced. However, no significant change was observed.

Another study involved the suppression of secondary electrons which could return to the source tube and heat it by bombardment. The grids used to suppress electrons reduced the total current about thirty percent when appropriate bias voltages were applied. The suppression of secondary electrons had a marked effect on the temperature of the source tube which no longer became red hot at high values of total current. But, again, the effect on the ratio of ion to droplet current was not significant.

A third arrangement involved the simultaneous application of direct and alternating voltages to the

droplet source tube. Positive voltages from 5.5 to 6.5 kv were combined with either 1.0 kv (RMS) at 30 megacycles or 1.5 kv (RMS) at 2 megacycles. With the direct voltage adjusted somewhat below the point where it was sufficient to operate the source, the addition of either alternating voltage caused the emission of droplets to occur. However, the ratio of droplet current to total current was not significantly different from the ratio obtained when operating with somewhat higher direct voltages and no alternating voltage.

A variety of changes were made in the geometry of the source tube as indicated in Section V A-1, but no significant changes in the ion to droplet ratio were observed.

The angular distribution from the tube and ball arrangement of Figure 2 was interesting in that it varied with total source current. When the current was below 60 or above 200 microamperes, particles and ions were emitted in substantial intensity over an entire hemisphere, but at intermediate values of total current, the emission was mostly in a forward cone with a half width of about 40°. The usual high ratio of ion current to droplet current prevailed at all values of the total current.

5. Massenfilter Studies of Ions

As trial-and-error methods had failed to disclose a variable which influenced the ion-to-droplet ratio significantly, the Massenfilter described in Section III B was constructed in the hope that more detailed studies of the distributions of charge-to-mass ratios of the ions and droplets would lead to a better fundamental understanding of the production process.

The first liquid metal investigated with the spectrometer was the mixture of bismuth, lead, and tin. The resolution was adjusted over a wide range but was never adequate to separate the isotopes of a single element or to separate lead ions from bismuth ions. Peaks in the collector current corresponding to the expected singly and doubly charged metal atoms were observed. In addition, a large number of peaks were observed and assigned to singly charged molecules or microdroplets containing several metal atoms.

In order to simplify the situation, it seemed desirable to work with a single element. Tin was selected and results were obtained during the infrequent occasions when the source operated properly. The liquid tin dissolved the stainless steel source tubes rather rapidly and made the accumulation of data difficult. However, six peaks were observed and assigned to Sn^{++}, Sn_2^+, Sn_3^+, Sn_4^+, and Sn_5^+. The peaks fell at the appropriate multiples of the Sn^+ peak with a precision of about one percent.

The destruction of source tubes by the liquid tin influenced a change to a eutectic mixture of lead and bismuth. The spread in isotopic weight of the isotopes of these two elements is actually smaller than the spread of the tin isotopes, so the fact that two elements are involved is not serious. The six strongest peaks again corresponded to singly and doubly charged atoms and singly charged molecules or microdroplets containing from two to five atoms. The two peaks following these six in intensity corresponded to two charges on molecules or microdroplets containing three and five atoms, respectively. Their intensity was a hundred times smaller than that of the peak

corresponding to singly charged atoms. The possibility that they resulted from impurities was eliminated by measurement of the charge-to-mass ratios with a precision of about 0.5 percent. In addition to the peaks already discussed, weak peaks were observed at charge-to-mass ratios corresponding to a single charge on molecules or microdroplets containing six and seven atoms. The intensities of peaks assigned to singly charged assemblies fell monotonically as the number of atoms increased. This decrease was fairly uniform and accumulated to a factor of fifty from single atoms to assemblies of five atoms. Then, the six atom peak was found to be a factor of ten lower than the five atom peak in intensity. Some evidence of extremely weak peaks corresponding to singly charged assemblies of eight to ten atoms was obtained.

Secondary electron emission was measured for a surface formed by the lead-bismuth metal on the collector of the spectrometer. The ion peaks corresponding to single charges on one, two and five atoms and double charges on one, three, and five atoms were investigated. The results showed that for all six peaks the secondary emission yields (secondary electrons per electric charge on the incident particle) were from 0.57 to 0.71 at 7.1 kv operating voltage. The investigation was not pursued to determine whether the observed differences were significant.

An attempt to study gallium was relatively unsuccessful as this source material dissolved the stainless steel source tubes at temperatures just above its melting point (30°C). However, two peaks were observed and identified as singly charged ions containing one and two atoms, i.e., Ga^+ and Ga_2^+.

The binding of the various singly charged assemblies of metal atoms (microdroplets) may involve some chemical forces but an additional effect is clearly present. This probably involves the force between the ionic charge and dipole moments present or induced in neutral atoms or molecules. The attraction between ions and neutral molecules is a well known effect which is observed, for instance, during the operation of a Wilson cloud chamber. On the other hand, the stability (for microseconds) of doubly charged configurations containing several atoms is difficult to explain.

6. Massenfilter Studies of Macroscopic Droplets

At charge-to-mass ratios below those where the ion peaks were observed, the transmitted current fell to a minimum and then rose to a broad continuum attributed to macroscopic droplets. The studies of the continuum were largely restricted to the eutectic mixture of lead and bismuth. Both open source tubes and the ball and tube arrangement were investigated. The charge-to-mass distributions were not greatly dependent on the type of source tube used.

Figure 18 shows some typical data obtained when the source was operating with the eutectic mixture of lead and bismuth. The plot shows the current transmitted through the spectrometer as a function of the charge-to-mass ratio selected. These data were obtained with a plain source tube having an inside diameter of 0.003". The results at 5.0 kv source potential show the current falling so slowly with decreasing charge-to-mass ratio that the mass was actually increasing. Hence, the

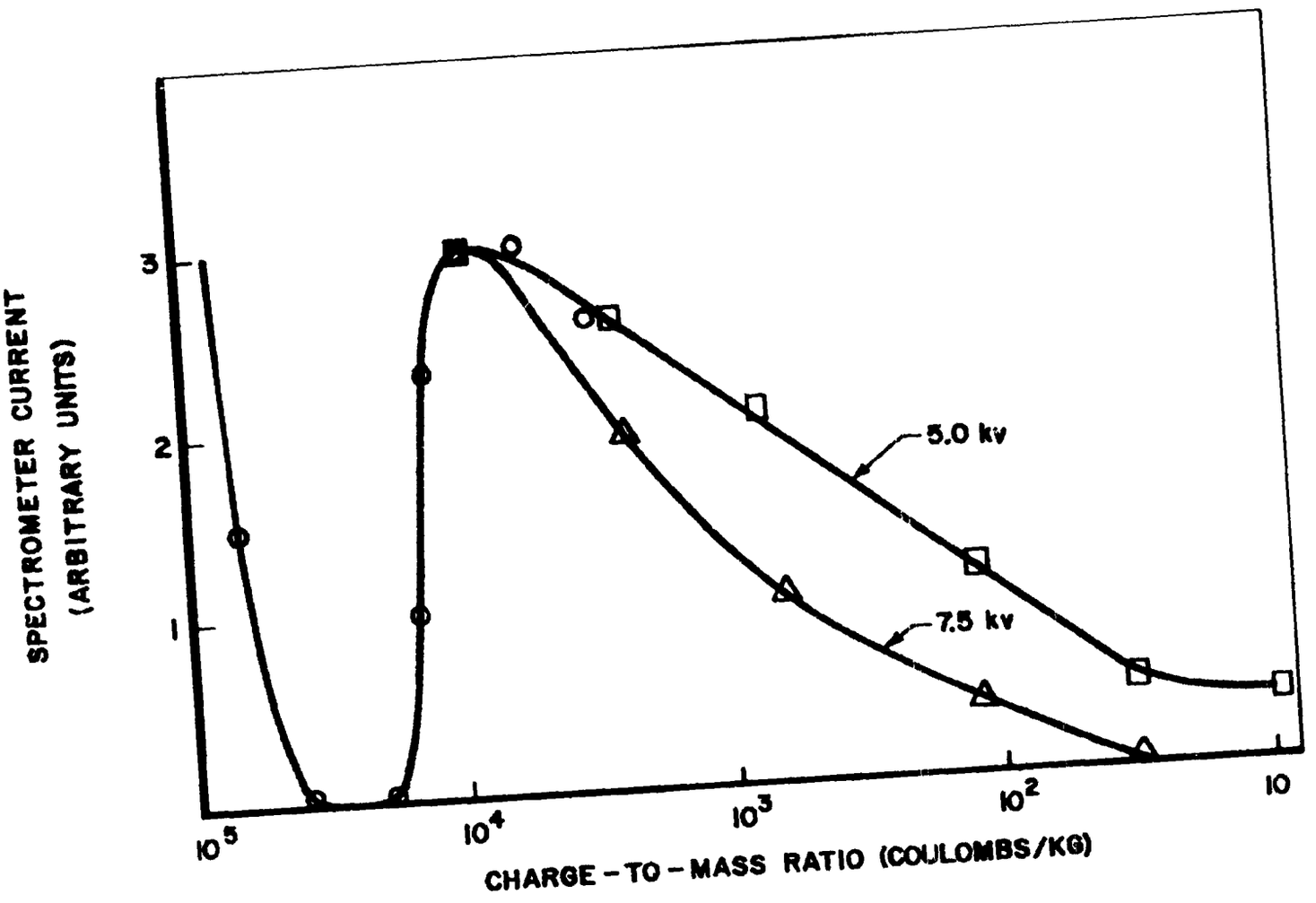

Figure 18. Charge/Mass Distribution of Metal Droplets.

greatest part of the mass was carried by large droplets with charge-to-mass ratios less than 10 coulombs/kilogram while the charge was mainly carried by small droplets having charge-to-mass ratios greater than 1000 coulombs/kilogram and by positive ions not shown in Figure 18. The distribution at 7.5 kv source potential falls more rapidly with decreasing charge-to-mass ratio and would still show a maximum if transmitted mass were plotted instead of transmitted current.

The points of Figure 18 at charge-to-mass ratios greater than 10,000 coulombs/kilogram (open circles) were obtained at an intermediate value of the source potential, 6.0 kv. They show the sharp decrease in intensity at 15,000 coulombs/kilogram and an increase toward the ion peaks which would appear to the left of the plot. Measurements at 5.0 and 7.5 kv to determine the position of the point of half-maximum on the decrease near 15,000 coulombs/kilogram indicated that this point fell 8 $\pm$ 6% higher in charge-to-mass ratio at 7.5 kv. This shift would hardly show on the charge-to-mass scale of Figure 18.

The cut off in the continuum at approximately 15,000 coulombs/kilogram was expected to occur at the point where the surface field on a droplet at the Rayleigh limit is sufficient to cause the field emission of ions (see Section IV A).

The assumption that the droplets of the continuum have charge-to-mass ratios close to the Rayleigh limit seems well justified in view of the results obtained while studying individual droplets (Figures 16 and 17). If this is indeed the case, the droplets at 15,000 coulombs/kilogram have a radius of 20 Å and a field at

their surface of 10^{10} volts/meter. Also, if this assumption is valid, we can assign a value of 10^{10} volts/meter for the field strength at which the field emission of ions occurs from the eutectic mixture of lead and bismuth. An attempt to observe a variation of this field strength with temperature failed to disclose a change. For this attempt the point of half-maximum near 15,000 coulombs/kilogram on curves similar to those of Figure 18 was determined at source temperatures of 143°C and 184°C. The difference in charge-to-mass ratio at the point of half-maximum was 3 $\pm$ 6%.

Measurements at 0°, 20°, and 40° with respect to the source tube established that the relative intensities of the ion peaks and various points on the continuous droplet distribution were relatively insensitive to the angle of emission.

The secondary emission yields were measured for lead-bismuth droplets and were found to be 0.13 $\pm$ 0.02 at 9400 coulombs/kilogram, 0.08 $\pm$ 0.02 at 700 coulombs/kilogram and 0.07 $\pm$ 0.02 at 33 coulombs/kilogram. Since the yields are charge ratios, they demonstrate that individual droplets could be detected by an electron multiplier.

7. Photomicrographs of Operating Source*

Figure 19 shows four photomicrographs of a source in a vacuum operating with Wood's metal as the working fluid. The source tube had an inside diameter of 0.005"

---

* These photographs were taken at the University of Illinois by A. Cho, and C. D. Hendricks.

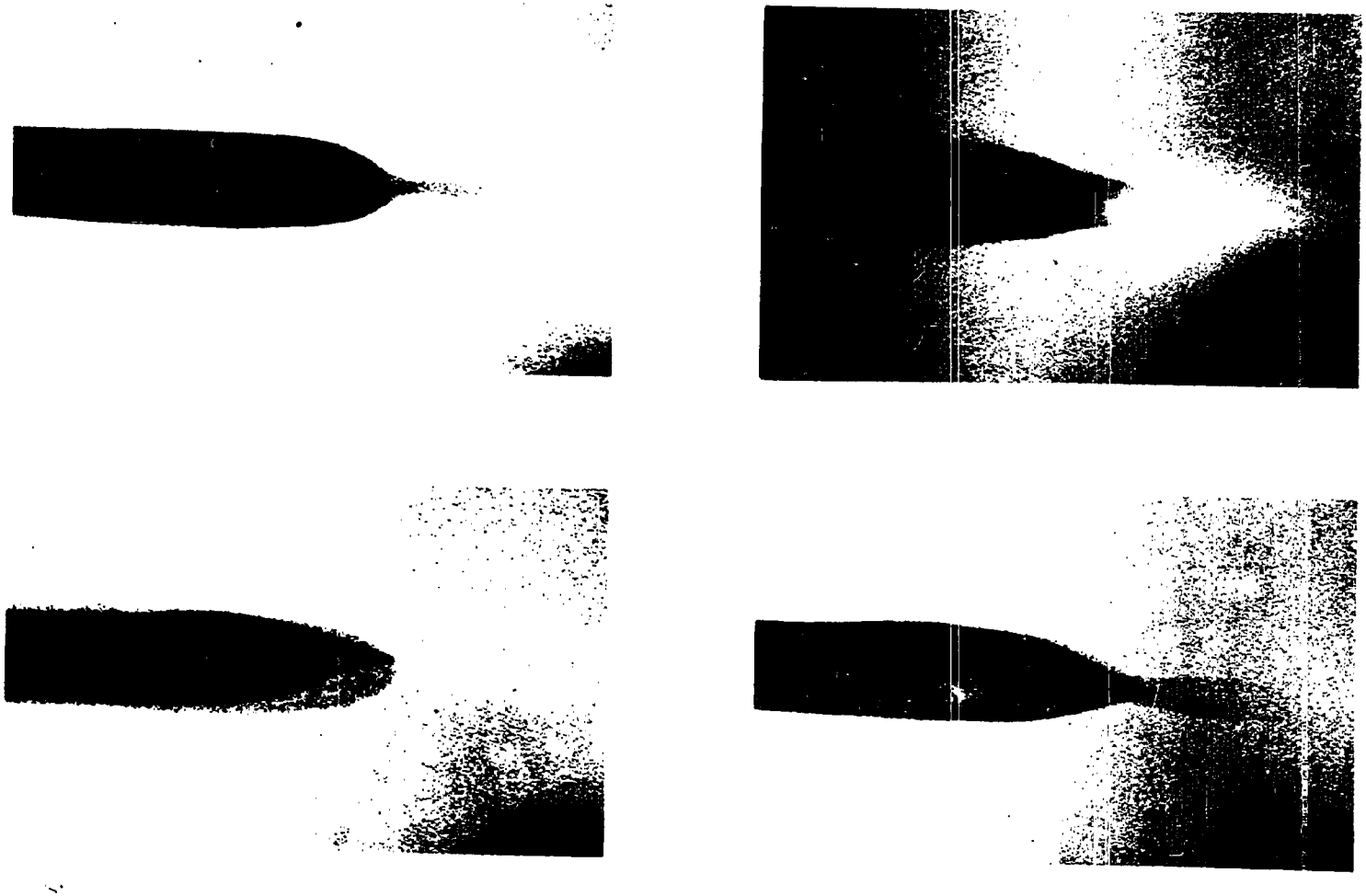

Figure 19. Photomicrographs of Source Operating With Woods Metal.

and was operated at a potential of 5.5 kv. These pictures show that the liquid metal forms a variety of tips as the source emits ions and droplets. Some of the photographs show two tip shapes as the result of double flashes from the xenon lamp used for illumination.

8. Electron Microscopy

Figure 20 is an example of the results obtained when metal droplets were examined by electron microscopy. Although the droplet size distribution may be distorted by the collection process, photographs of this type are of value in that they provide a clear demonstration that many extremely small droplets are produced. The scale of the figure is approximately one micron/inch and the smallest particles one would expect to find on a basis of the Massenfilter data (20 A radius) would appear as 0.004" spots in the photograph. We believe the electron microscope results give a qualitative confirmation of our interpretation of the other data.

B. Fused Salts

When Draw-temp 275 was used as the working fluid and the Massenfilter used to study the output of the source, the only output observed was a large current of ions emitted in a broad cone in front of the source tube. The ratio of droplets, if any, to ions was clearly smaller than the ratio observed with metals.

C. Organic Liquids

1. General

Two modes of operation have been observed when an organic liquid or an organic liquid containing added ionic conductors isused as the working fluid. Most of

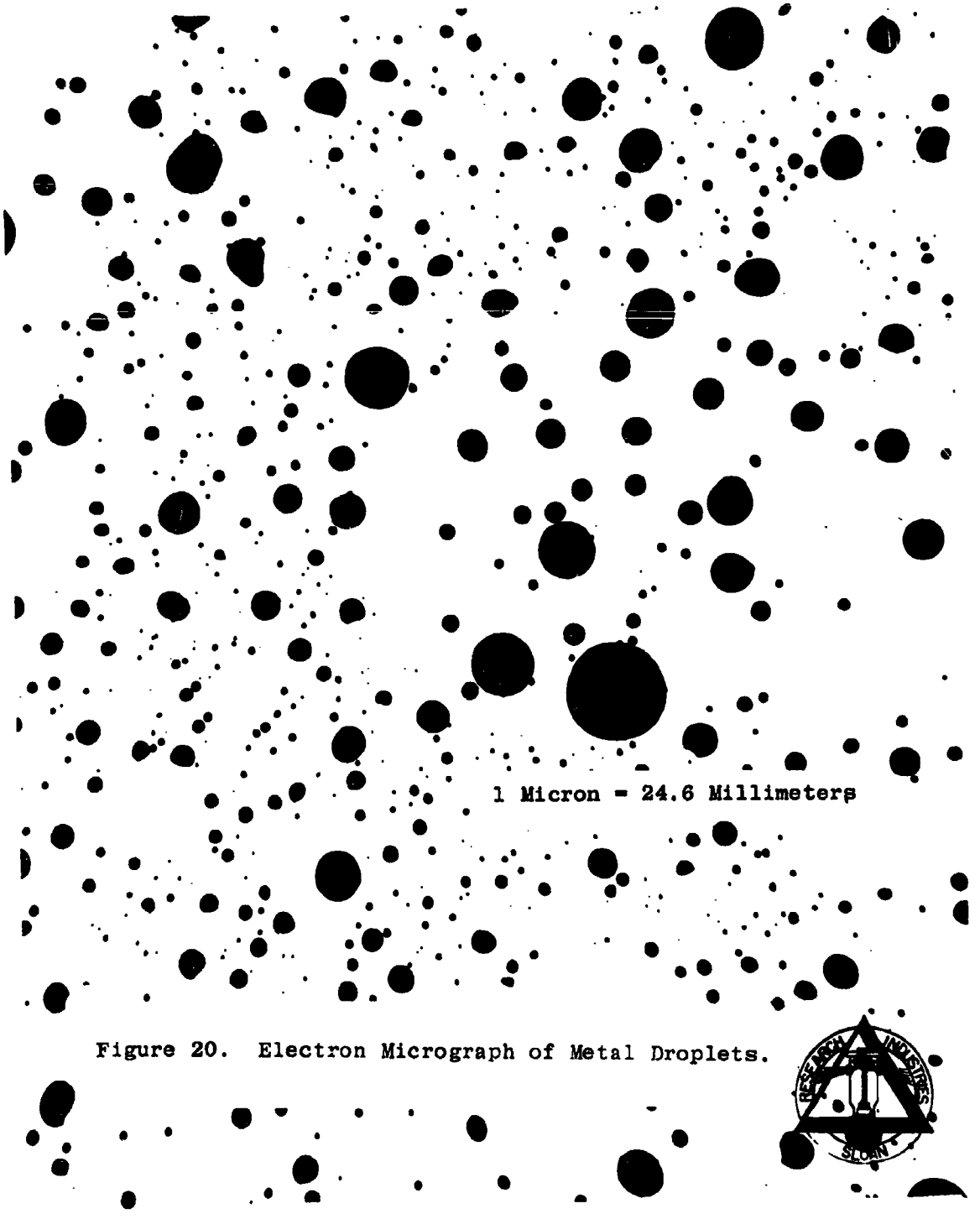

Figure 20. Electron Micrograph of Metal Droplets.

the liquids can be used to produce either of the modes. In one of the modes, discrete jets of charged droplets are emitted at various angles. In some cases, a small current of ions is emitted into the jets along with the droplets. In the other mode of operation, ions of the working fluid are emitted into a broad cone in front of the source tube. Charged droplets may be present in this mode, but they have not been detected. With liquids of low conductivity, e.g. octoil, the ion mode occurs at a higher source voltage than the droplet mode. As one proceeds to liquids of higher conductivity, there is a tendency for both modes to occur at lower voltages with the threshold voltage of the ion mode dropping more rapidly than the thresnold voltage of the droplet mode. In the case of glycerol with added antimony trichloride which is the combination giving the highest conductivities among the organic liquids studied in the present work, we are unable to acnieve stable operation in the droplet mode at antimony trichloride concentrations above about seven percent. Apparently, the ion mode has a lower threshold than the droplet mode at concentrations appreciably higher than this.

When operating in the droplet mode the total source current is about one microampere whereas in the ion mode the current tends to be hundreds of microamperes.

The present studies have concentrated on investigation of the droplet mode of operation.

2. Single Droplet Studies

Octoil was used as the working fluid with a 0.005" open source tube for studies with a single particle detector. Figure 21 is a plot of the charge-to-mass ratios

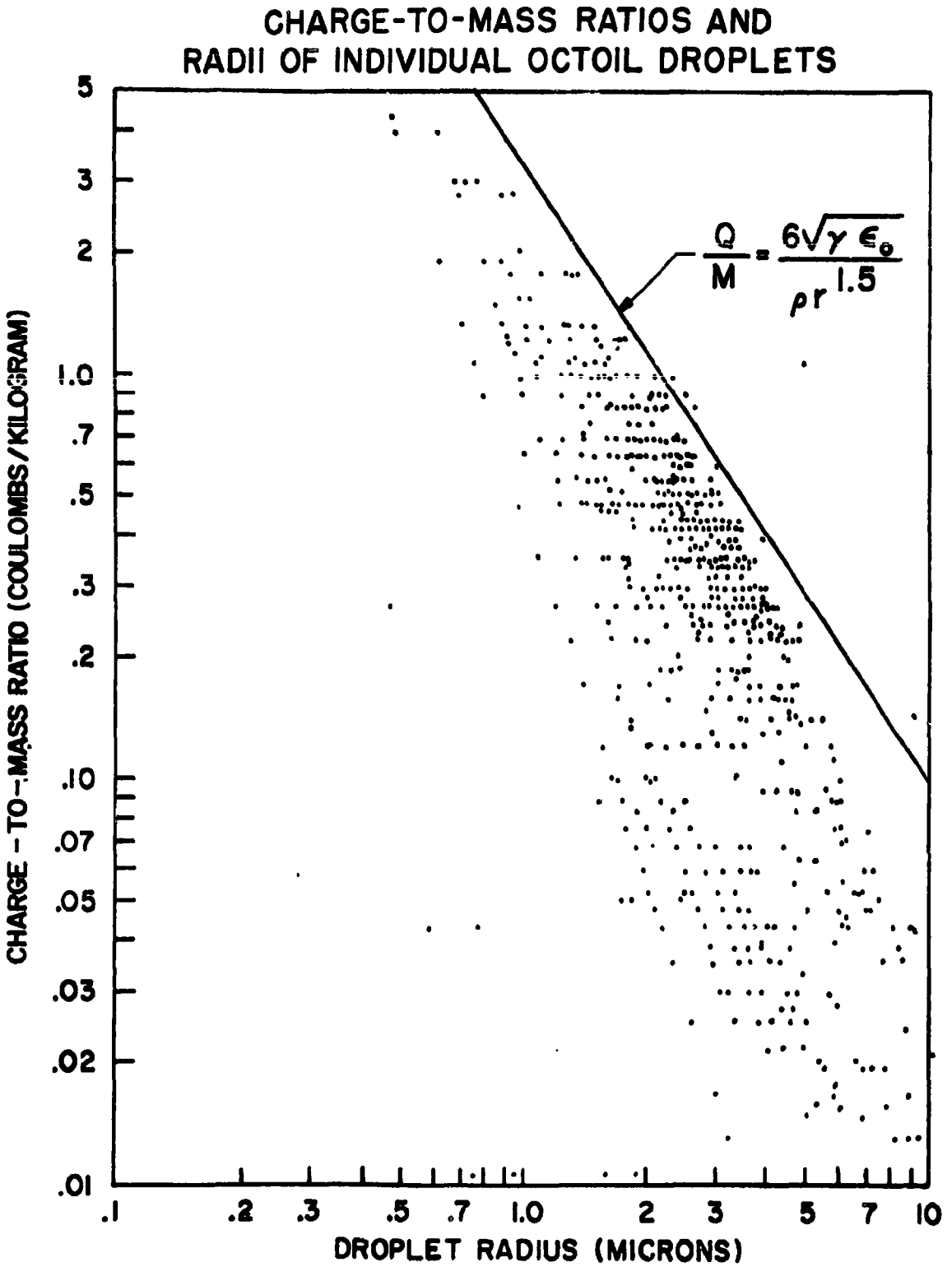

Figure 21. Charge/Mass Ratios and Radii of Individual Octoil Droplets.

and radii of the individual droplets observed. About 0.3 percent of the data fall above the Rayleigh limit, but this is probably the result of experimental errors[5]. The limit of detection at the time these data were taken was 10^{-15} coulombs and would appear on the plot as a line of slope -3 to the left of which very few droplets were re-corded. The tendency of the droplets to acquire charges close to the Rayleigh limit is clearly demonstrated. Figure 22 is a histogram of the number of droplets observed as a function of droplet radius. The radius of 2.3 microns at the center of the large peak of the histogram is about what we would predict from Massenfilter data taken at a later time. Octoil has a resistivity of 4×10^{7} ohm cm.

3. Massenfilter Results

When octoil from a 0.005" open source tube was investigated with the Massenfilter, the transmitted current showed a narrow peak at 0.75 coulombs/kilogram. If this peak were the result of droplets charged to the Rayleigh limit, their radius would be 2.6 microns. Alternatively, if the peak were caused by droplets with a radius of 2.3 microns (as suggested by the single droplet measurements), they would need a charge 20 percent below the Rayleigh limit in order to account for the charge-to-mass ratio observed with the Massenfilter. The narrow peak observed with the Massenfilter leads us to believe that the distribution of radii must be narrow, and that the distribution observed with the single particle detector (Figure 14) was probably broadened by variations in the operating conditions of the source during the accumulation of data. Fortunately, the Massenfilter data are taken rapidly so that instrumental broadening is not a serious problem.

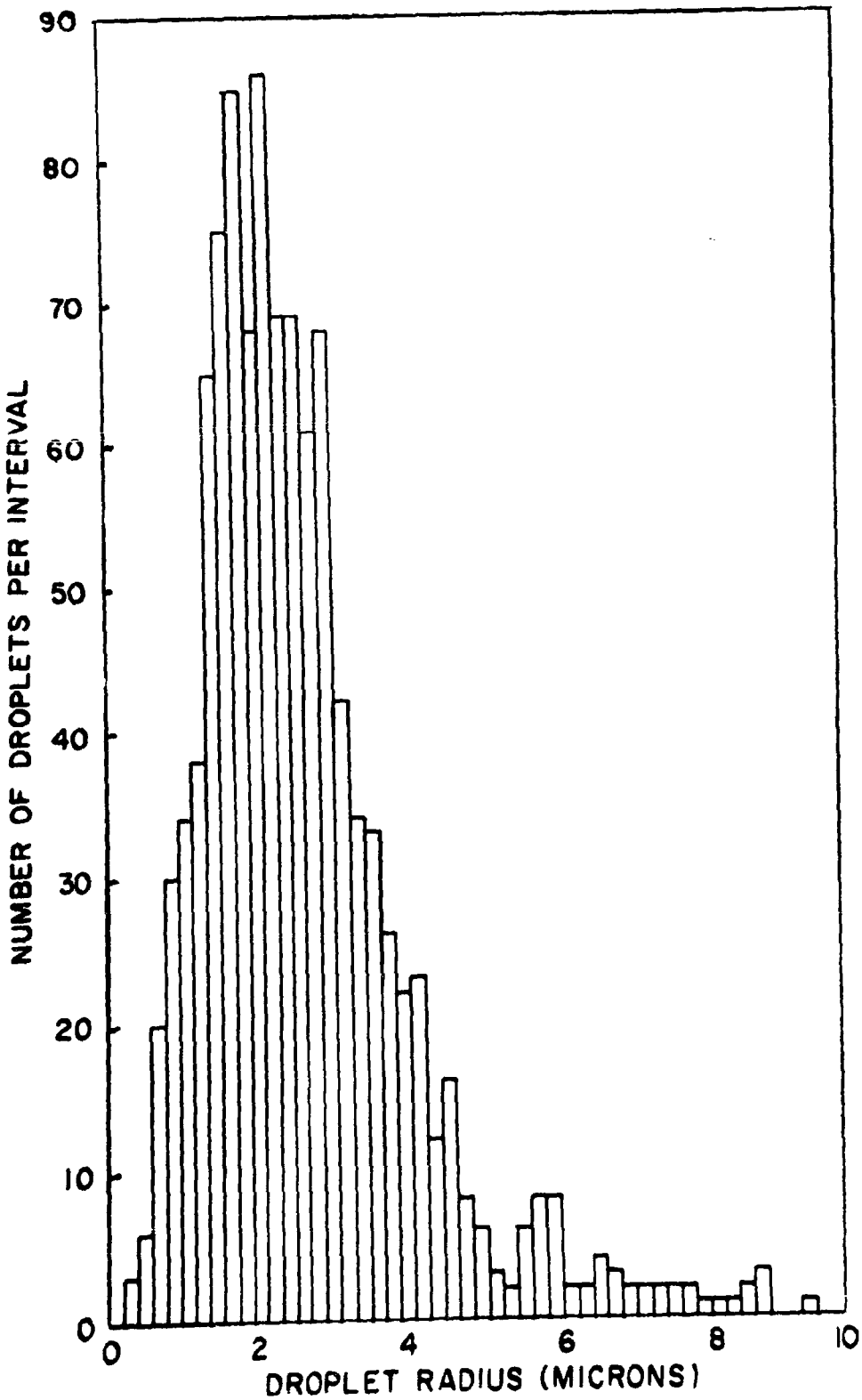

Figure 22. Histogram of Octoil Droplet Radii.

Conductivity measurements were made for octoil, glycerol, and silicone oil with various ionic conductors dissolved in them. The latter included antimony trichloride, urea mononitrate, tetra-n-butyl ammonium picrate, and hydroquinone. The combinations showing relatively high conductivity were selected for study with the Massenfilter. In general, narrow distributions of the charge-to-mass ratio were found in all cases investigated and higher charge-to-mass ratios were observed from solutions of high conductivity. The highest conductivities and the highest charge-to-mass ratios were obtained with various concentrations of antimony trichloride in glycerol, and this combination was selected for more extensive study. It was found that the stability of source operation could be improved by using 0.010" source tubes packed with Fiberfrax at the emitting end, and this arrangement was used for the studies of this working fluid. Somewhat more recent work has indicated that sintered nickel tubes might prove more reliable. These results are discussed further along in this report. In order to obtain antimony trichloride concentrations greater than about four percent by weight, it was necessary to warm the glycerol and operate the source at a slightly elevated temperature. Hence the reservoir was held at 35°C for the higher concentrations. With the lower concentrations it was determined that raising the source temperature to 35°C did not seriously affect the results.

Figure 23 shows the charge transmitted through the Massenfilter as a function of charge-to-mass ratio for a 3.5 percent solution. The operating voltage was 10.0 kv. From the distribution of current as a function

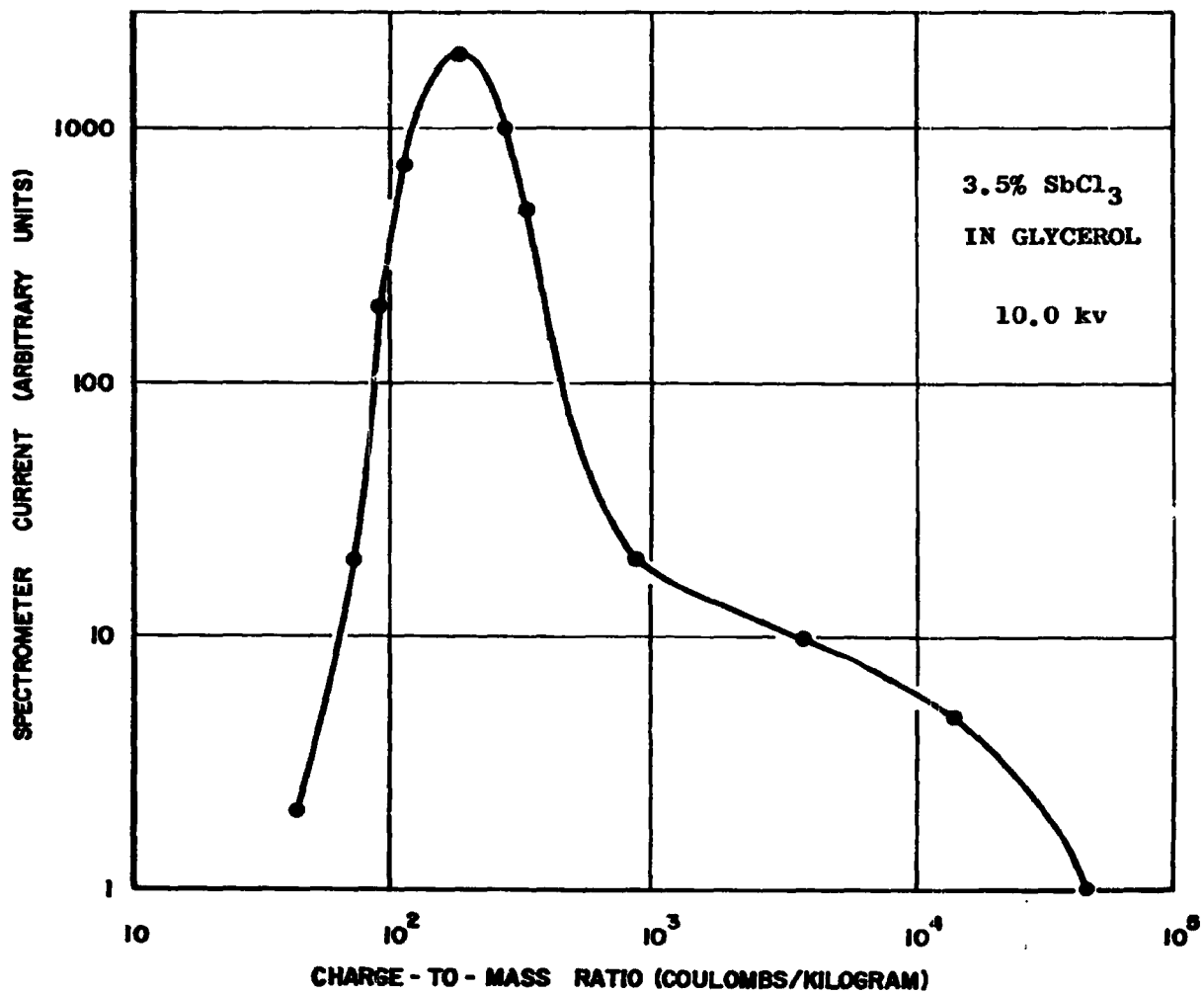

Figure 23. Total Charge versus Charge-toMass Ratio for Glycerol containing 3.5% Antimony Trichloride.

of charge-to-mass ratio, one can calculate the distribution of mass (Appendix A). This distribution is shown in Figure 24 which demonstrates that the tail of the current distribution at high charge-to-mass ratios is drastically reduced when one looks at the mass distribution. The curve of Figure 24 and Hunter's formula[6] have been used to calculate the loss of thrust which would occur if droplets having this distribution were used in an electrostatic propulsion system in place of particles having a single value of the charge-to-mass ratio. The result indicates that less than one percent having this distribution were used in an electrostatic propulsion system in place of particles having a single value of the charge-to-mass ratio. The result indicates that less than one percent of the thrust would be lost.

It is of interest to note that for glycerol droplets at the peak of the distribution of Figure 23 (180 coulombs/kilogram), the Rayleigh limit is such that the maximum possible droplet radius is 730 Å and the maximum possible charge is 3.7×10^{-16} coulombs.

The intensity of the peak of Figure 23 rises and falls two decades within a single decade of charge-to-mass ratio. This curve is typical of the results obtained with 3.5 percent solutions of antimony trichloride in glycerol, but we are not able to reproduce the position of the peak by attempting to achieve the same operating conditions. The peak position has been observed to vary from 180 to 330 coulombs/kilogram.

The curve of Figure 25 is a distribution of charge-to-mass ratios observed when operating with

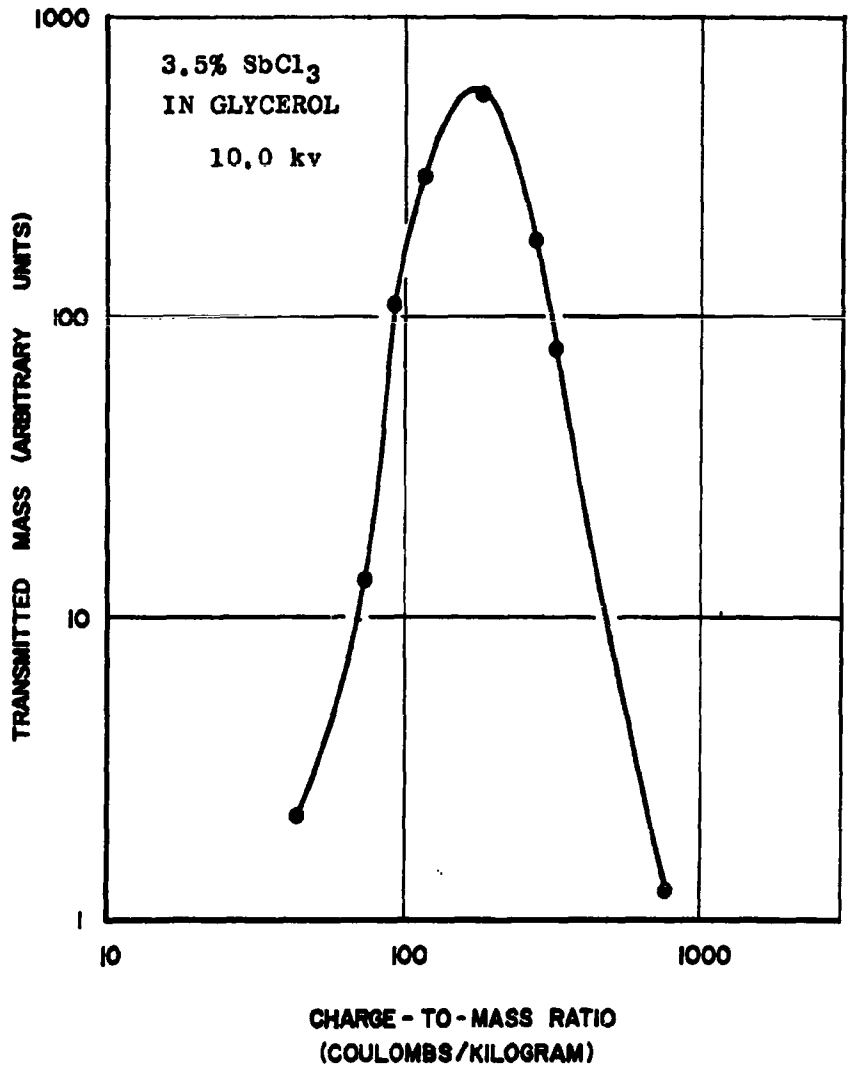

Figure 24. Total Mass Vs. Charge/Mass Ratio of Glycerol Containing 3.5% Antimony Trichloride.

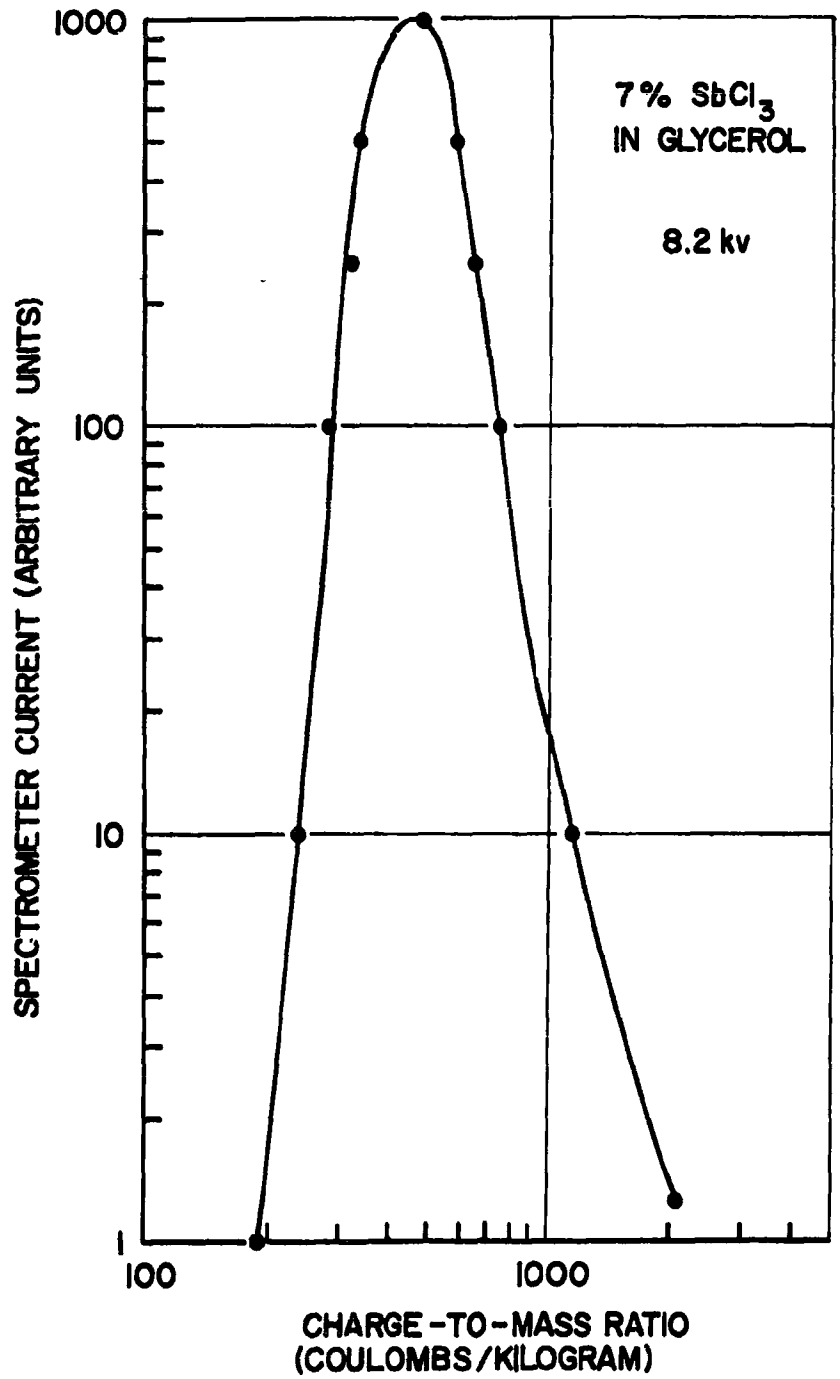

Figure 25. Total Charge Vs. Charge/Mass Ratio of Glycerol Containing 7% Antimony Trichloride.

seven percent by weight of antimony trichloride in glycerol. The peak of the curve is at about 470 coulombs/kilogram. If the droplets at the peak of this curve are charged to the Rayleigh limit, their radius is 390 $\mathring{A}$ and their charge is 1.4×10^{-16} coulombs.

While it has not been difficult to adjust the glycerol point emitter so as to observe a charge-to-mass peak of the desired type in the Massenfilter, the status is still that of a sensitive laboratory experiment requiring constant attention. The total beam current from the point emitter is remarkably stable. The current through the Massenfilter is less so.

A major uncertainty and a major problem exists because the glycerol point emitter sends out several beams of droplets simultaneously. These beams may exist anywhere in a cone of 60° total angle. The ability to rotate the point emitter about one axis confines the exploration of droplets to a line scan. A drawing of the jet pattern is shown in Figure 26A and 26B. Photographing these pattern formations is somewhat difficult because of the low contrast between droplet clumping and background and also because the low yield (mass) in some of the jet beams evaporate. Cooling the receiver helps considerably by reducing the evaporation rate.

In principle, if we know q/m, the flow rate $\frac{m}{t}$, and the current q/t, we can write the equation

$$I = q/t = q/m \times \frac{m}{t}$$

(A) SINTERED NICKEL TIP

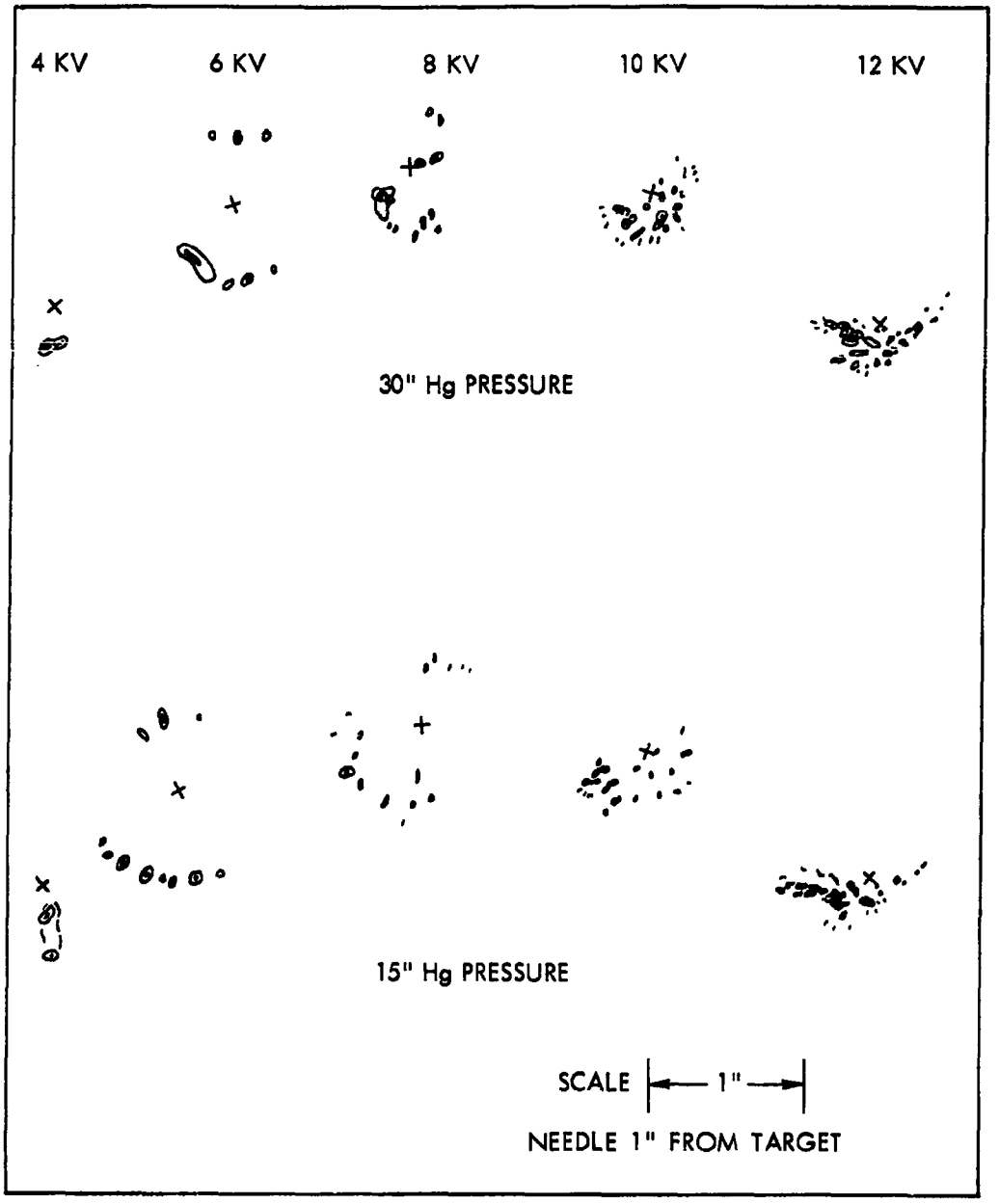

Figure 26A. Jet Patterns, Sintered Nickel.

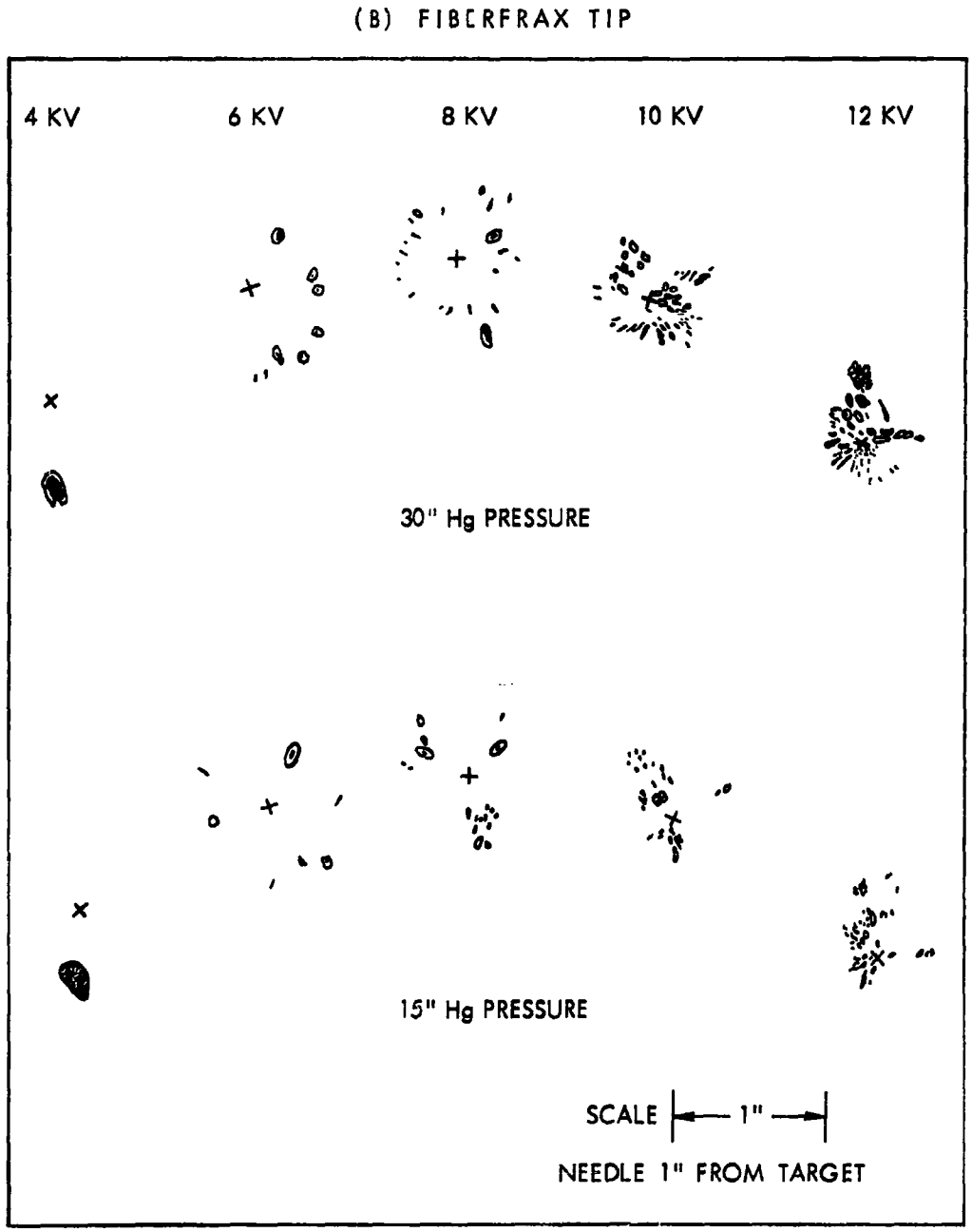

Figure 26B. Jet Patterns, Fiberfrax.

A series of measurements of these quantities are given in Table 1. It can be seen that the current calculated from the flow rate and peak charge/mass observed are of the same order of magnitude as the current measured on a meter. Considerably additional work is necessary along these lines.

A systematic study of the influence of the parameters source voltage and source pressure (mass flow rate) upon the resulting observable charge/mass was made. This is shown in Table 2. This data was taken for a Fiberfrax packed .010 inch inside diameter stainless steel needle. The glycerol-antimony trichloride fluid had a resistivity of 4200 ohm cm. It is felt that 5000 ohm cm represents a higher limit for charge/mass investigation for the region in which we are interested. The resistivity is also a more pertinent parameter than weight ratio. However, it is observed that the resistivity has on occasion increased as much as 25% with time, a phenomenon to be investigated. At each voltage setting we looked for charge/mass peaks and also the half power points. Runs were made from 4 kv to 11 kv and then the source pressure was charged. In all cases, with one exception no other peaks or ions were observed.

Volts $X10^3$	Flow Pressure Inches Hg	Droplet Current $X10^{-6}$ amps	Needle Current $X10^{-6}$ amps	q/m coul/Kg	$\dot{m}$ Kg/sec	Calculated Current $X10^{-6}$ amps
8	10	.2	.3	330	$.6x10^{-9}$	.198
8	10	.2	.3	380	$.6x10^{-9}$	.228
8	5	.2	.3	440	$.4x10^{-9}$	.176
8	10	.5-1.0	.6-1.25	270	$.6x10^{-9}$	.162

TABLE 1.

NEEDLE CURRENT AS A FUNCTION OF

CHARGE TO MASS AND MASS FLOW

TABLE 2

Pressure Inches Hg	Volts KV	Coul/Kg 1/2	Coul/Kg Peak	Coul/Kg 1-1/2	
1	4		None		No ions or other peaks
	5		None		" "
	6		None		" "
	7		100		" "
	8	115	155		Adjacent peak at 210 coul/kg
	9	260	370	600	Less than 1% ions
	10		None		No ions or other peaks
	11		None		" "
5	4		None		No ions or other peaks
	5		None		" "
	6		None		" "
	7	<50	<50	<50	" "
	8	89	94	125	" "
	9	82	140	205	" "
	10	100	165	265	" "
	11	215	260	360	" "
15	4		None		No ions or other peaks
	5		None		" "
	6	<50	<50	<50	" "
	7	245	520	1250	" "
	8	<50	<50	<50	" "
	9	58	120	175	" "
	10	<50	78	125	" "
	11		None		" "

TABLE 2 (CONTD)

Pressure Inches Hg	Volts KV	Coul/Kg 1/2	Peak	1-1/2	
30 (1 atmosphere)	4		None		No ions or other peaks
	5		None		" "
	6		<50		" "
	7		<50		" "
	8		<50		" "
	9		<50		" "
	10	broad	76	broad	" "
	11	68	105	155	" "

At one inch of Hg pressure and nine KV, a peak was observed at 370 coulombs/kilogram. A very small peak, much less than 1%, was observed at 330,000 coulombs/kg. At 15" Hg and 7 K.V., a peak was observed which appears to be too high in comparison with the rest of the data. In general however we observe that at a given voltage, increasing the source pressure (mass flow rate) decreases the charge/mass. When we keep the pressure constant, an increase in voltage increases the charge/mass.

Considerably more data of this type should be obtained, using source fluids of different conductivity and sintered nickel point emitters.

The problem of homogeneity of droplet jets was approached in the following manner. Using zero bias containment (Appendix A) a jet was obtained for which most of the current was found to be in an interesting

range, (e.g. 200 coulombs/kilogram). The D. C. bias was inserted and the jet examined for peak charge/mass and ion current. The most persistent ions obtained occur at 355,000 coulombs/kilogram. At a source point position giving a peak, little ion current was obtained as shown in the table below for position A. If the needle is now rotated a few degrees, with the Massenfilter tuned for ions, 355,000 coulombs/kilogram, a new position of the point emitter is found which is rich in this narrow ion region and has a low value of charged droplets. For this position identified as B, the axis of the hollow needle point emitter nearly always makes a larger angle with the axis of symmetry of the Massenfilter than does position A.

10 KV Source Voltage, 20" HG Pressure, 6000 ohm cm oil, 0.92 μ.a. Beam Current

Q/M coul/kg	I_{MF} x 10^{-10} amps	Position
210	8.0	A
355,000	0.14	A
210	8.0	A
355,000	0.14	A
350,000	0.34	B
210	No Peak	B
355,000	0.32	B
210	No Peak	B

Q/M coul/kg	$I_{MF} \times 10^{-10}$ amps	Position
210	5.2	A
355,000	0.14	A
210	5.6	A
355,000	0.16	A
355,000	0.32	B
210	No Peak	B
355,000	0.35	B
210	No Peak	B

Although 210 coulombs/kilogram is listed for position B, the no peak value under Massenfilter current means that the non ion current was very much less, about 1%, than the ion current between a charge/mass ratio extending from less than 50 coulombs/kilogram up to several thousand coulombs/kilogram, the region of interest. The ion current is not corrected in this table for the band width of the Massenfilter (Appendix A). Such a correction would decrease its influence radically in both positions A and B. This experiment was repeated several days later with similar results. It should be noted that the fluid, identified as 6000 ohm cm resistivity was originally measured as 4200 ohm cm.

11.75KV Source Voltage, 16" Hg Pressure, 6000 ohm cm oil, 0.25 μ.a. Beam Currents

Q/M coul/kg	I_{MF} x 10^{-12} amps	Position
125	1.8	A
355,000	0.15	A
125	1.7	A
355,000	0.12	A
350,000	2.0 No other peaks	B
125	2.8	A
355,000	0.1	A
355,000	1.3 No peaks	B B
125	2.0	A
355,000	0.1	A

Recently an 0.010 inch inside diameter sintered nickel needle was inserted into the system and utilized for obtaining charged droplets. The peak current was relatively stable and illustrated in Figures 27, and 28. Figure 27 contains the raw data, uncorrected for band width. Figure 28 has the same data but is corrected for the varying band width as described in Appendix A. The ordinate axis now has dimensions kilograms/sec. The ion current in the corrected data is down by three orders

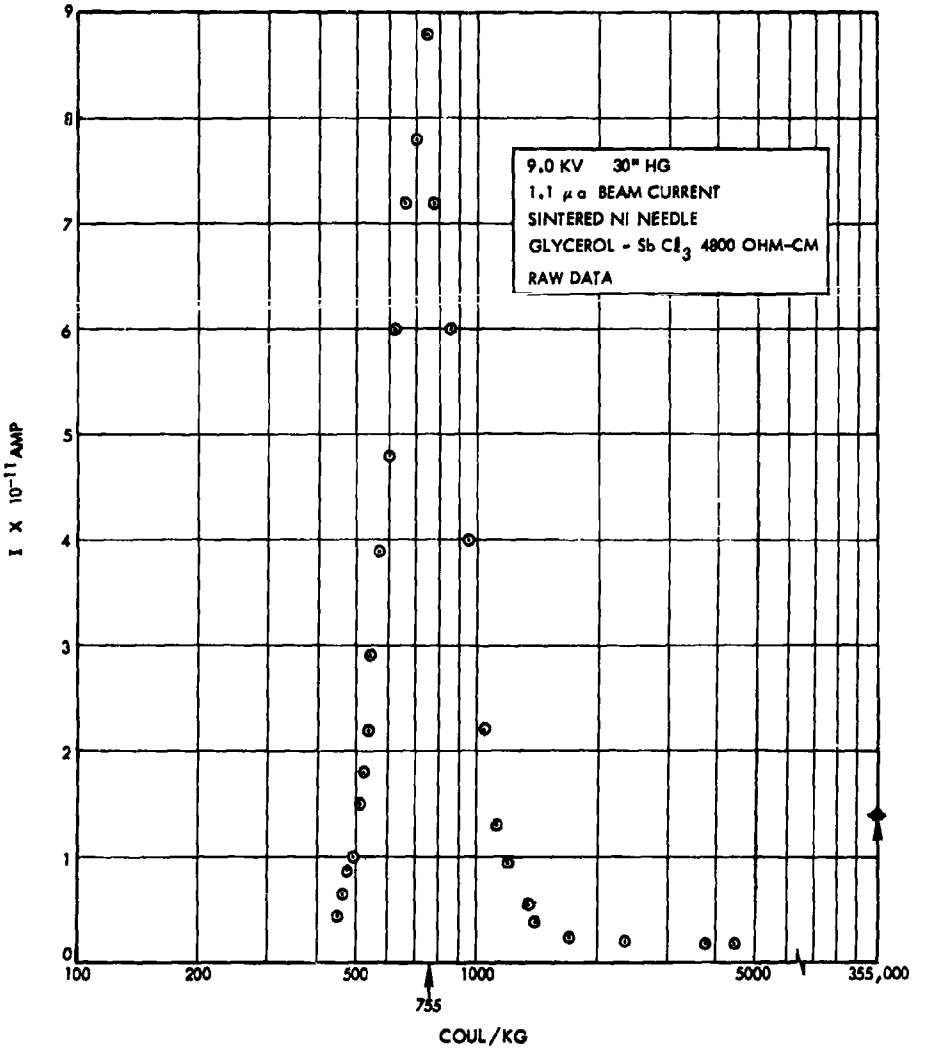

Figure 27. Q/M for Sintered Needle.

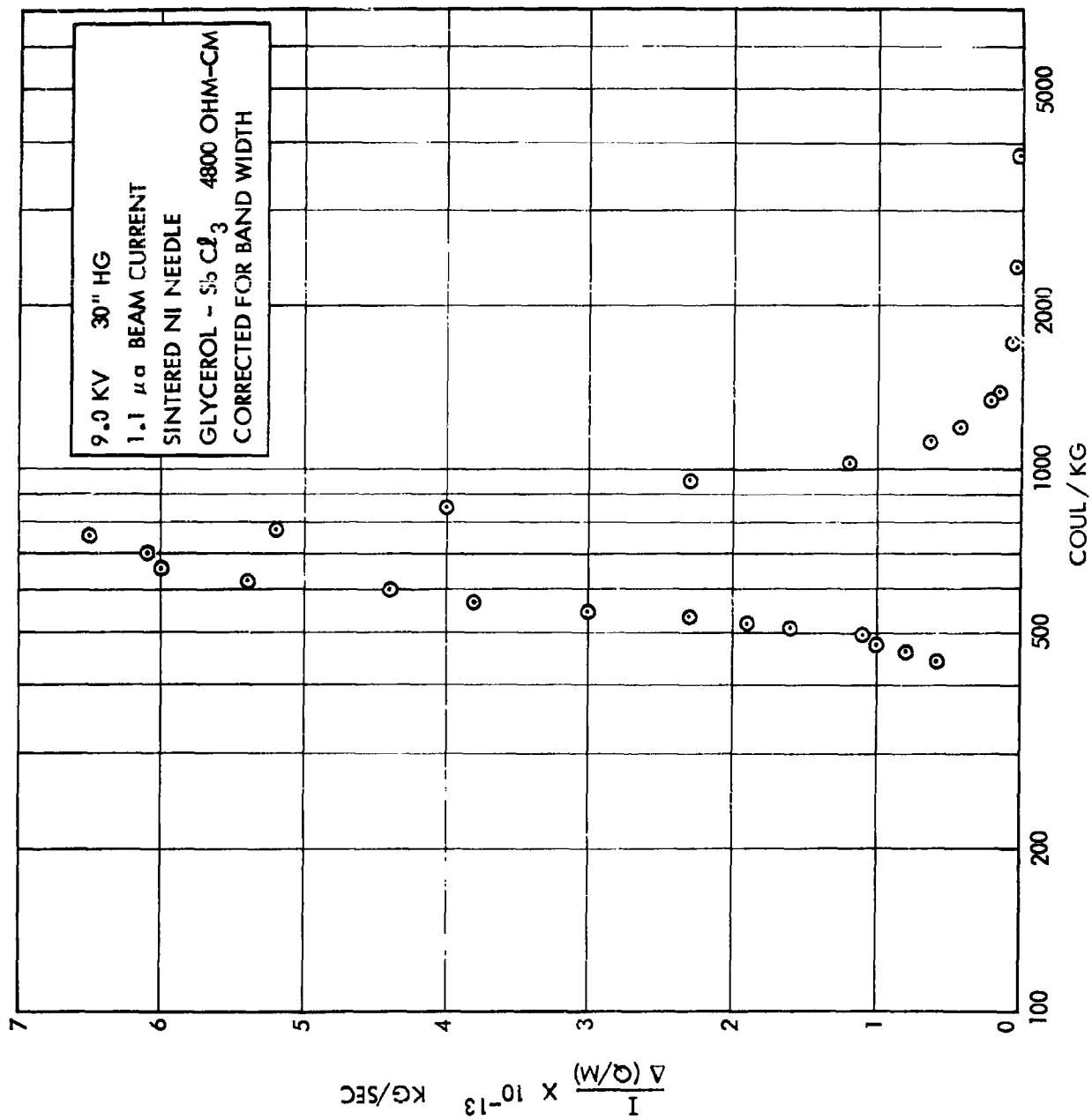

Figure 28. Corrected Mass Flow for Sintered Needle.

of magnitude and not shown on the graph. Our peak occurs at 755 coulombs/kg.

In a paper by R. E. Hunter[6], the efficiency of a heavy particle ion engine with a distribution of charge-to-mass is shown to be

$$\left[\frac{\overline{\frac{1}{C^2}}}{\overline{C}}\right]^2$$

where C refers to the charge/mass ratio, the bar sign indicating the appropriate average. Using the data of Figure 27, these terms were evaluated and the efficiency was found to be just better than 98%.

Some attempts have been made to identify the persistent ion peak at 355,000 coulombs/kg. Several possibilities are given in the table below.

A.	1 Glycerol molecule, singly charged (ion)	1,040,000 coul/kg
B.	2 Glycerol + 3 Sb^{++}	330,000
C.	3 Glycerol + 2 Sb^{++}	349,000
D.	5 Glycerol + 3 Sb^{+++}	347,000
E.	3 Glycerol + 1 Sb^{+++}	361,000
F.	3 $Glycerol^{+}$	347,000

If we assume that we know the position of the 355,000 coul/kg ion to $\pm$ 5%, we may rule out the single charge glycerol molecule and the 2 glycerols plus three Sb with one antimony doubly charged. As a matter of fact the glycerol ion, case A, is easily identified by the Massenfilter. It is normally much weaker than the ion in question. Not enough is yet

known concerning the other possibilities listed which would enable identification to be made.

Little has been said about charge/mass below 50 coulomb/kg. Evidence points to the fact that this range is relatively easy to obtain and is shown on Table 2. Evidently ions are no problem here.

4. Photomicrographs of Operating Source

For a 0.005" source tube with octoil as the working fluid, Figures 29 to 35 show the tip of the source tube, and in some cases, the emitted droplets at source potentials from two to six kilovolts. The development of smaller droplets and an increasing number of jets as the voltage is raised is clearly shown by this series of photographs. At the low operating voltage used for these photographs, droplets of very low charge-to-mass ratio are produced. At voltages where high charge-to-mass ratios prevail, the details of the filaments emitting jets of droplets would not be resolved in the photomicrographs.

Figures 29 to 35, as well as Figure 19, were obtained by C. D. Hendricks and his collaborators at the University of Illinois working under a subcontract.

VI. DISCUSSION OF RESULTS

A. Summary

A general survey of the ions and charged droplets emitted from a point source, under a variety of operating conditions has been accomplished. It has been shown that the conductivity of the working fluid is of prime importance in determining whether charged droplets can be produced without a large number of ions accompanying them and that the

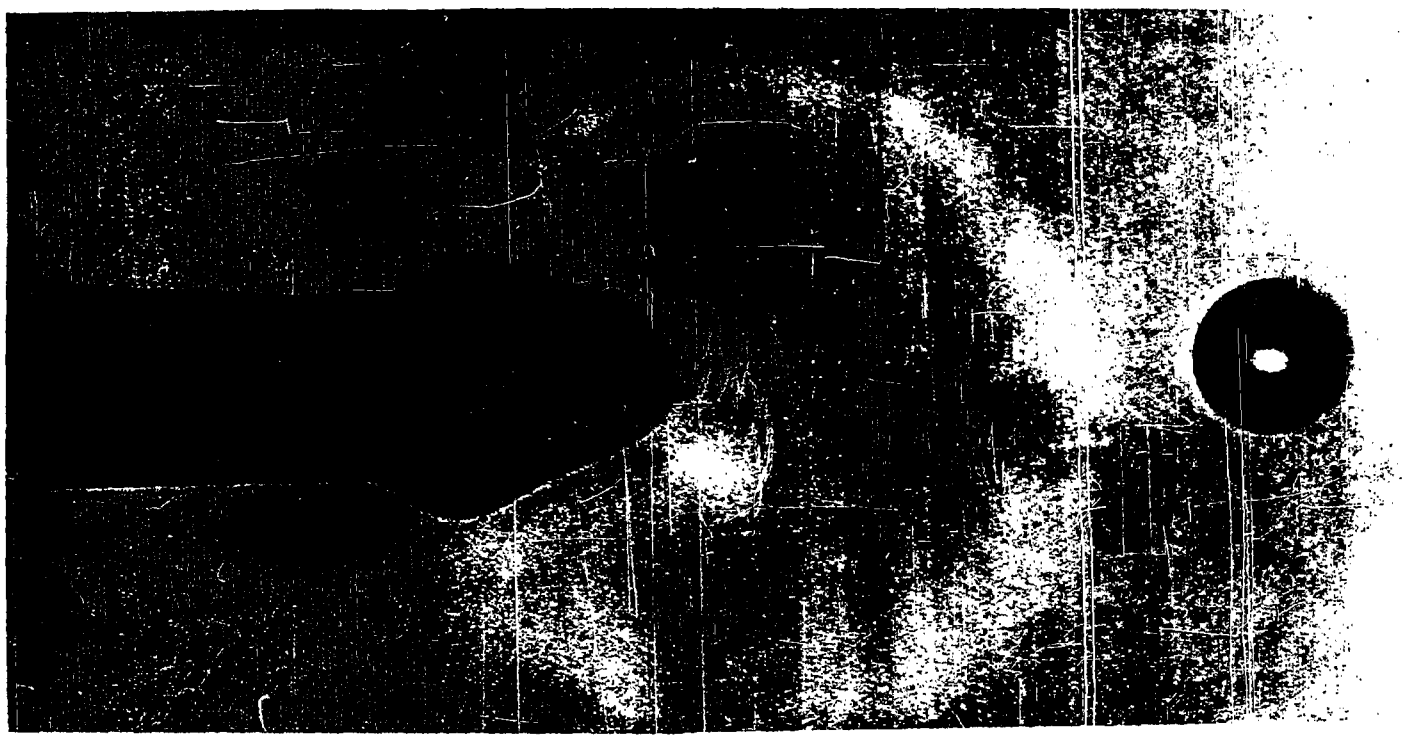

Figure 29.

Scale
5 Mils

Working Fluid: Octoil-S
Accelerating Voltage: 2000 volts
Diameter of Capillary: 5 mils
Reservoir Pressure: 1 cm Hg.
Chamber Pressure: 6×10^{-6} mm Hg.

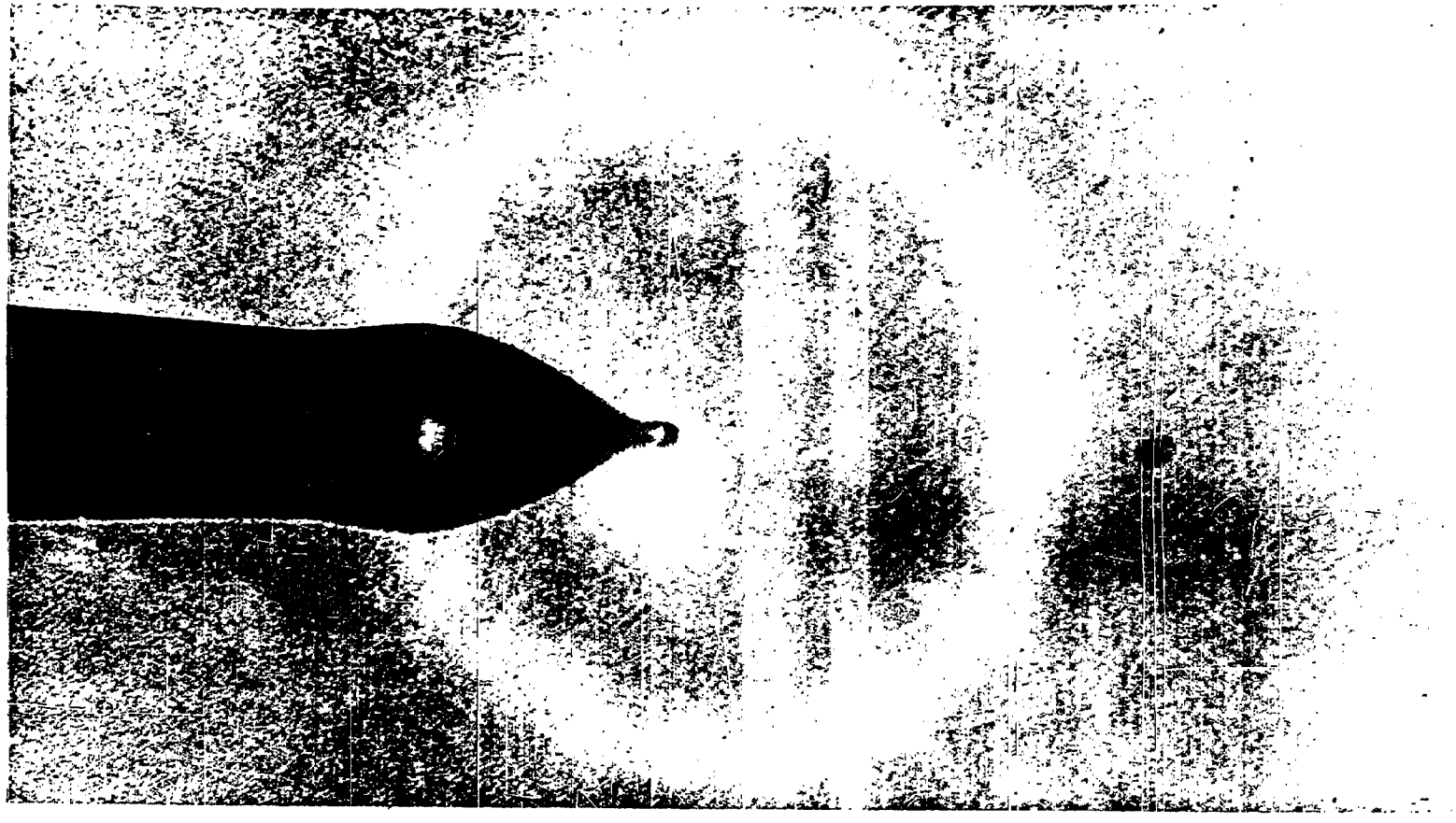

Figure 30. Working Fluid: Octoil-S
Accelerating Voltage: 2500 volts
Diameter of Capillary: 5 mils
Reservoir Pressure: 1 cm Hg.
Chamber Pressure: 6 x 10-6 mm Hg.

Scale
5 Mils

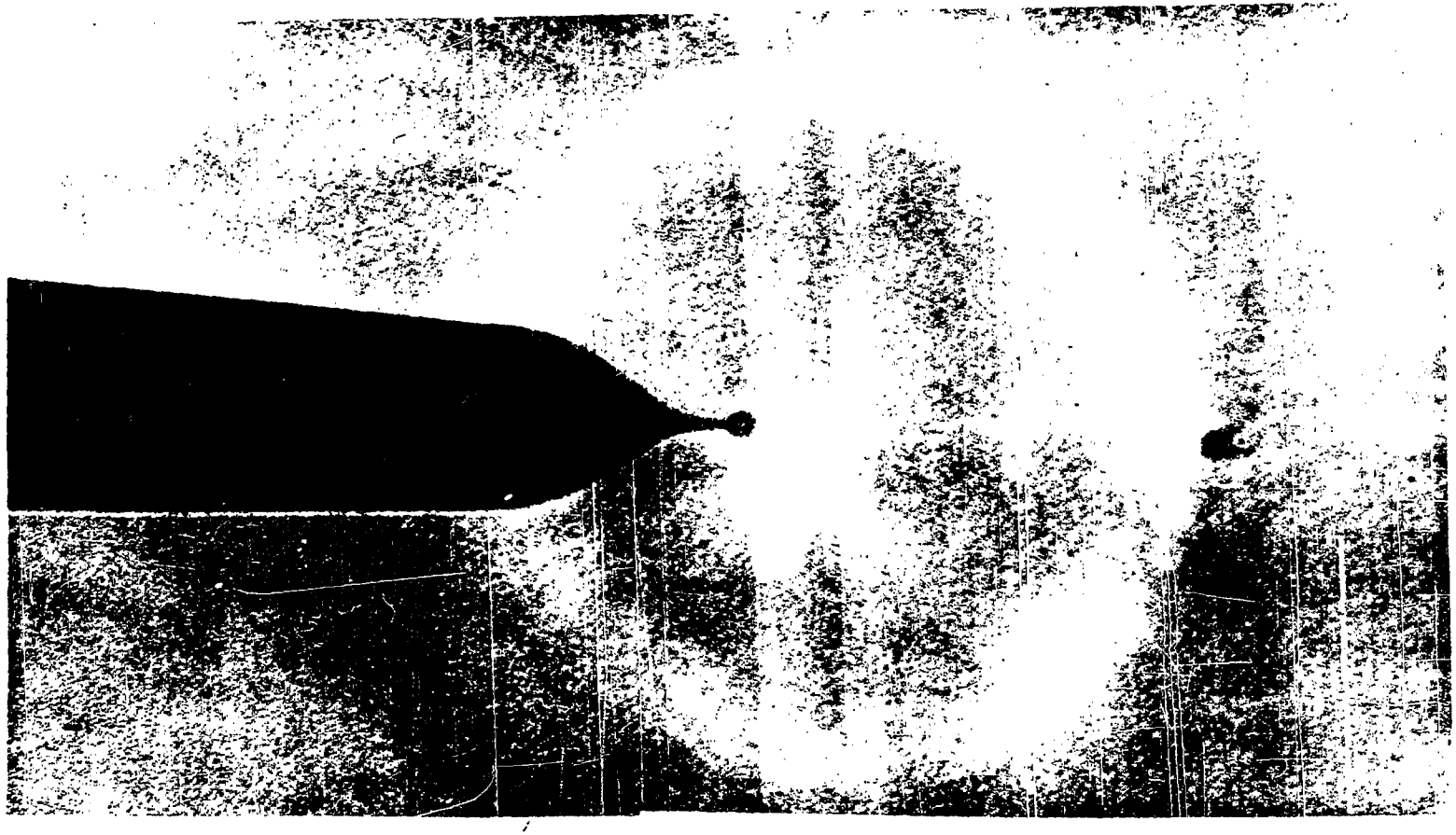

Figure 31. Working Fluid: Octoil-S
Accelerating Voltage: 2500 volts
Diameter of Capillary: 5 mils
Reservoir Pressure: 1 cm Hg.
Chamber Pressure: 6×10^{-6} mm Hg.

Scale
5 Mils

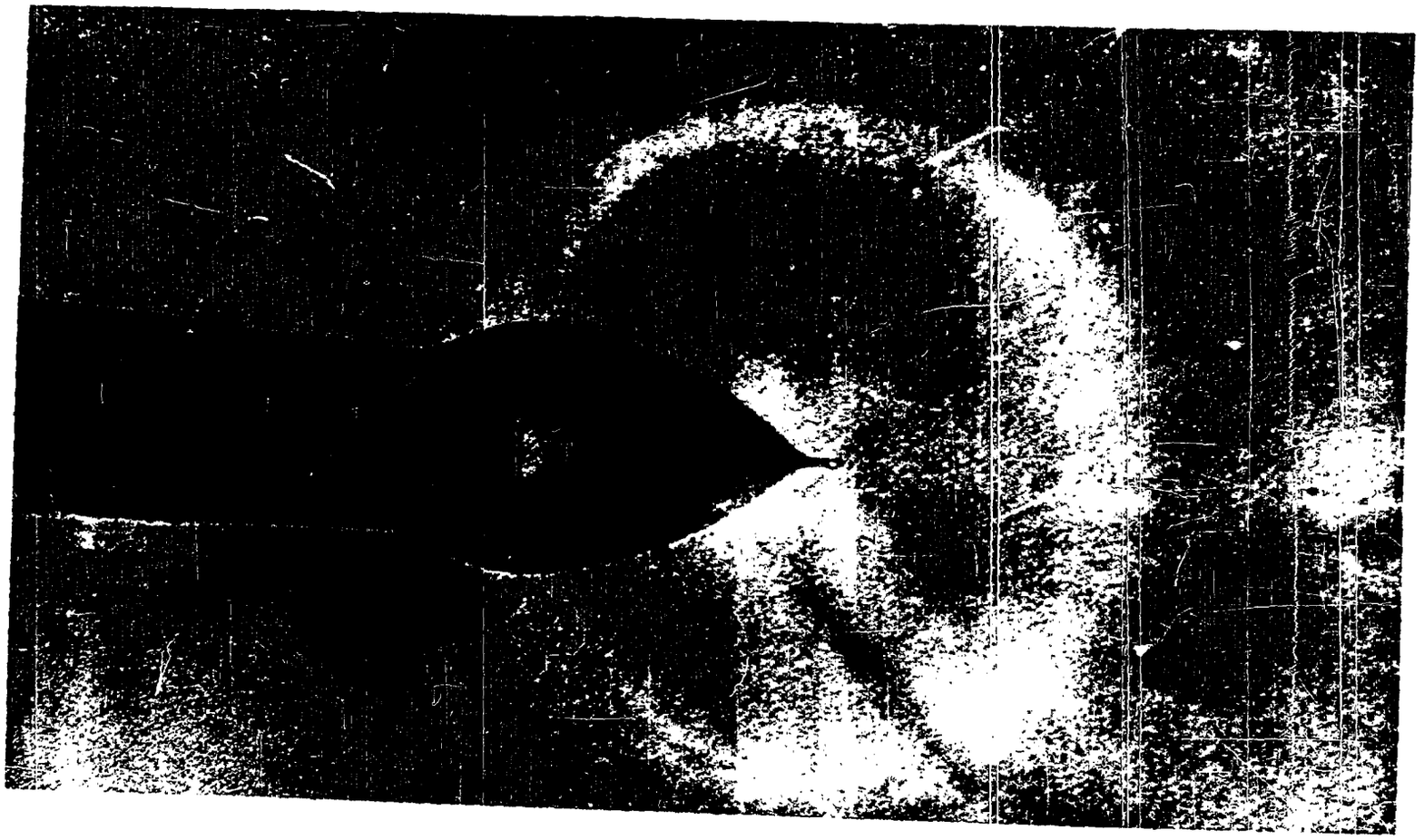

Figure 32. Working Fluid: Octoil-S
Accelerating Voltage: 3500 volts
Diameter of Capillary. 5 mils
Reservoir Pressure: 1 cm Hg.
Chamber Pressure: 6×10^{-6} mm Hg.

Scale
5 Mils

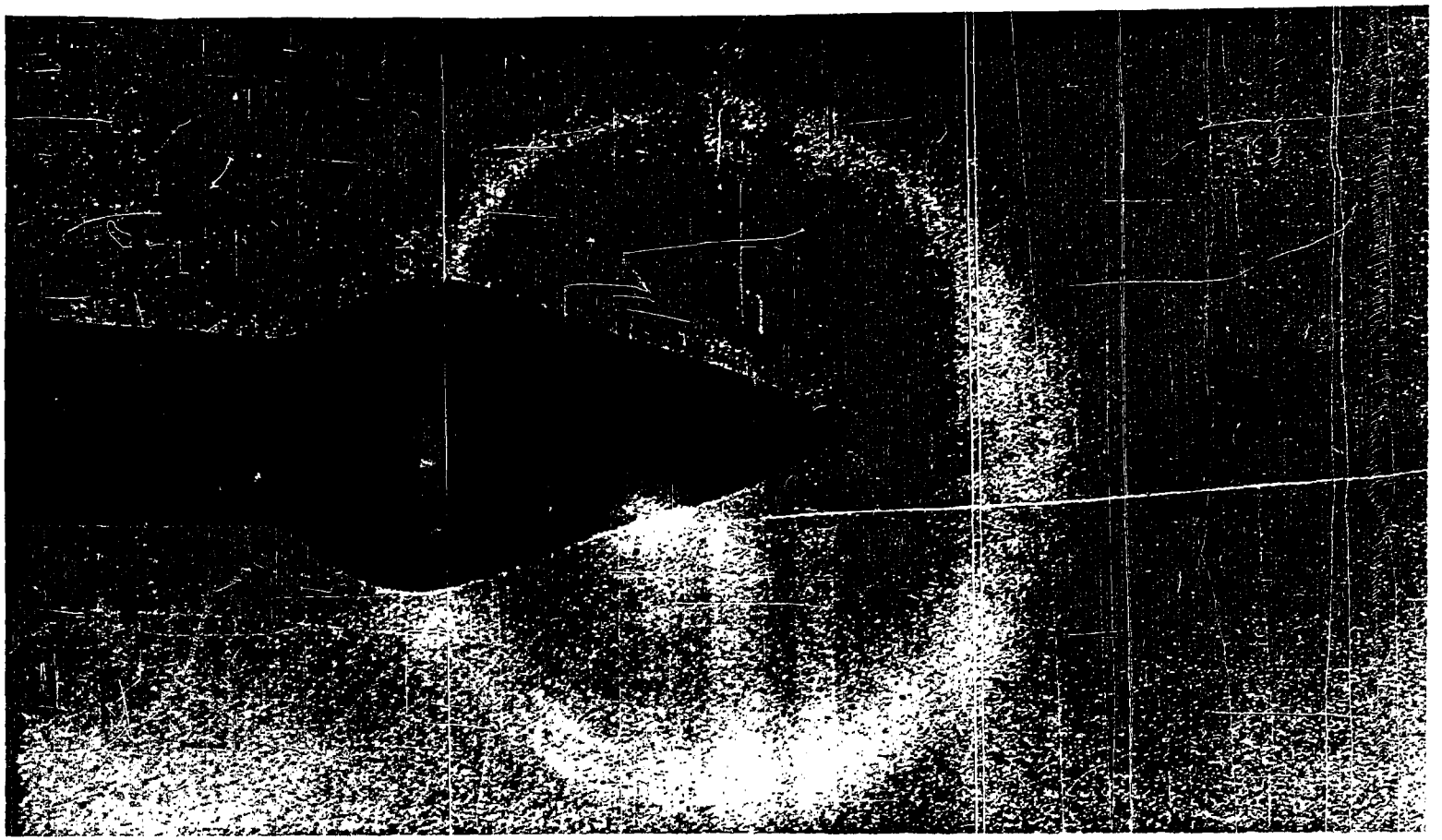

Figure 33. Working Fluid: Octoil-S
Accelerating Voltage: 3500 volts
Scale — Diameter of Capillary: 5 mils
5 Mils — Reservoir Pressure: 1 cm Hg.
Chamber Pressure: 6×10^{-6} mm Hg.

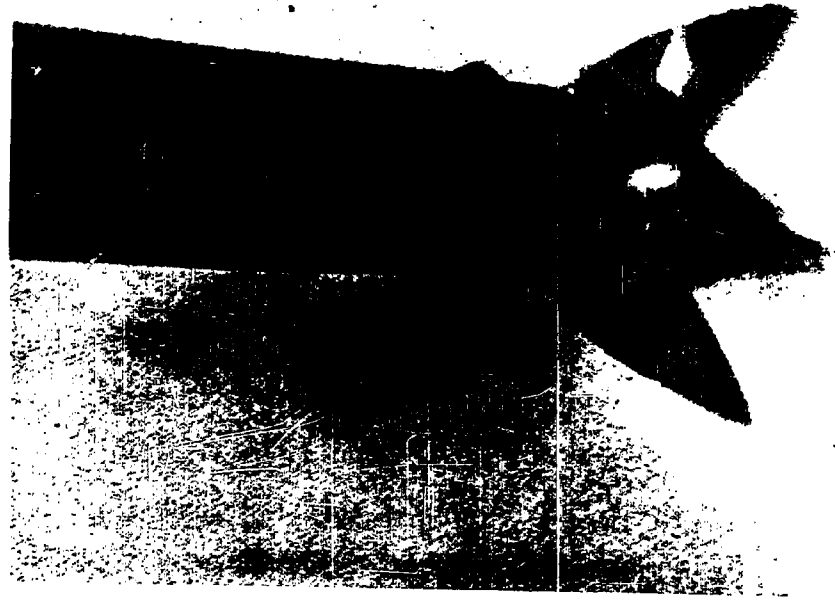

Figure 34. Working Fluid: Octoil-S
Accelerating Voltage: 5000 volts
Diameter of Capillary: 5 mils
Reservoir Pressure: 1 cm. Hg.
Chamber Pressure: 6×10^{-6} mm Hg.

Scale
5 Mils

Figure 35. Working Fluid: Octoil-S
Accelerating Voltage: 6000 volts
Diameter of Capillary: 5 mils
Reservoir Pressure: 1 cm Hg.
Chamber Pressure: 6×10^{-6} mm Hg.

Scale
5 Mils

conductivity is also of great importance in determining the charge-to-mass ratio of the droplets.

The theoretical limitations on the maximum charge that a droplet of given size can carry, the Rayleigh limit and the ion limit, have been pointed out and confirmed partially.

The possibility of using a source of the type investigated to study the field emission of ions from a liquid metal has been pointed out. An approximate value of 10^{10} volts/meter has been inferred for an eutectic mixture of lead and bismuth.

Some interesting positive ions containing up to seven metal atoms have been discovered and investigated.

Charged droplets of uniform charge-to-mass ratio and with few or no ions accompanying them have been produced with charge-to-mass ratios as high as 755 coulombs/kilogram.

REFERENCES

1. Paul, W., M. Raether, Z. Physik 140, 262 (1955)

2. Muller, E. W., "Field Desorption" Phys. Rev 102, 618-624 (May 1956)

3. Lord Rayleigh, Phil. Mag. 14, 184 (1882)

4. Langmuir, D. B., and Yeh, G. C. K., "A simple physical interpretation of Rayleigh's formula for instability of charged droplets", Ramo-Wooldridge Research Laboratory internal report RW-RLM-203, (May 26, 1960)

5. Hendricks, C. D., Jr., "Charged Droplet Experiments", J. Colloid Science, 17 No. 3 (March 1962)

6. Hunter, R. E., "Theoretical Considerations on Non-Uniformly Charged Expellant Beams", ARL TN 60 136 (August 1960)

APPENDIX A

Massenfilter

1. Resolution and Bandwidth

The resolution of the Massenfilter shown in Figure 9 was obtained with an accelerating potential of 1000 volts on the potassium ions. This condition leads to an experimentally evaluated resolution $m/\Delta m$ of 50. For any other accelerating potential U, the resolution will differ, being greater for lower values of accelerating voltage. Paul shows an empirical equation which relates the number of cycles an ion undergoes in the Massenfilter to the resolution.

$$n = 3.5\sqrt{\frac{m}{\Delta m}}$$

but f cycles/sec x t secs = n

n = number of cycles in Massenfilter
f = frequency of R.F. Field
t = time in Massenfilter
L = length of Massenfilter
U = accelerating voltage on ion
V = peak R.F. voltage on rails
r = field radius

now $t = \dfrac{L}{\sqrt{2U\ e/m}}$

Therefore $n = \dfrac{fL}{\sqrt{2U\ e/m}}$

but $.706 = 4\ \dfrac{e\ V}{mr^2 4\pi^2 f^2}$ (stability condition for the Mathieu equation)

or $f = \sqrt{C\ e/m\ V}$ where $C = \dfrac{1}{.706\pi^2 r^2}$

and $n = \dfrac{\sqrt{C\ e/m\ V\ L}}{\sqrt{2\ e/m\ U}}$

this can be reduced to

$$n = K\sqrt{\frac{V}{U}}$$

hence

$$\frac{\left(\frac{m}{\Delta m}\right)_o}{\left(\frac{m}{\Delta m}\right)_1} = \frac{U_1}{U_o}$$

Letting

$R = \frac{M}{\Delta M}$, we have

$$R_1 = \frac{R_o U_o}{U_1}$$

This equation not only permits us to know the resolution of the Massenfilter for any accelerating potential of our ions but also brings to light a further important consideration. As we examine higher and higher charge/mass ratios our spectrometer samples an increasing bandwidth of charge-to-mass. The optical analogy is an opening of the spectrometer slit. When we rewrite the equation above we obtain

$$\Delta(Q/M) = \frac{1}{R}\frac{Q}{M}\frac{U_1}{U_o}$$

When U_o = 1000 volts, R = 50 and now expressing U_1 in kilovolts, then for our instrument

$$\Delta(Q/M) = .02\,\frac{Q}{M}\,U_1$$

Data reported on in the past has in general not made use of this expression. For example Figure 18 and 23, contain plots of spectrometer current vs. charge/mass which are uncorrected for the increase in slit width. Applying the bandwidth correction to these curves would simply diminish the effect of the higher charge/mass ratios with no shift in the position of the peak. This is in part shown for figure 24. The correction here has been accomplished by dividing the Massenfilter current by the corresponding charge/mass. In Figures 27, and 28, uncorrected and corrected data are graphed. The dimensions obtained by dividing current by bandwidth, $i/\Delta(q/m)$, are amperes per unit coulomb/kilogram or simply kilograms/sec.

2. Zero Bias Containment

An additional mode of operation of the Massenfilter is feasible if we remove the D.C. bias on the rails of the spectrometer. This has the effect of decreasing the constant a in the Mathieu equation to zero and permits all charged particles or ions to be stable out to the "q" value of 0.908.

Since "q" is defined as

$$q = 4\frac{Q}{M}\frac{V}{4\pi^2 f^2 r^2}$$

then $(Q/M)_L = kf^2$, the highest Q/M which will be contained by the quadrupole

The constant k is known from the instrument parameters. The term $(Q/M)_L$ gives us the maximum charge/mass for which the instrument is stable. All charge/mass below that value will also be stable. The problem is somewhat more complicated than the above statements indicate for the "degree of stability" varies being greatest for that charge/mass which corresponds

to q equal to 0.706, and dropping off for low values. Therefore as $(Q/M)_L$ is extended by an increase in the frequency, the containment of low charge/mass particles suffers, and is a complicated function of the entrance conditions of the particles into the Massenfilter.

Nevertheless zero bias containment allows a fast qualitative scan to be made of charged particle emission. By switching frequency bands, the change in current indicates immediately where the majority of charge carriers exist. An increase in current in going from low to high frequencies always indicates the existance of ions. However when charged droplet peaks exist, the total current starts decreasing after switching past the "stable" band.

APPENDIX B

ANALYSIS INVOLVING SPACE CHARGE LIMITATION AND MECHANISM OF DROPLET FORMATION

The current that can be drawn from a single needle is limited by space charge. A sizable field must exist in order to form droplets; the charged particles in transit tend to shield the needle and reduce the field. We will now estimate the current that will produce this shielding.

One method of deriving this current is by recognizing that thrust is produced by field lines of force terminating on charges in transit (thereby accelerating them) rather than on the needle. Therefore the reduced force on the needle due to the reduction of field can be equated to the thrust. Let us calculate the current that will reduce the field by two when the charge is emitted from a point into an angle θ. The initial force on the surface, of radius r, subtended by the emitting point is,

$$F = \frac{\theta^2 r^2 \epsilon_o E^2}{2}$$

Because of the presence of the needle shank and other geometrical factors,

$$E = k \frac{Vapp}{r} \quad \text{where k is about 0.2}$$

The change of force due to the reduction of field is $F_o - F_1$, where F_1 is due to E/2

$$\Delta_F = \frac{3}{8} \theta^2 k^2 \epsilon_o \, Vapp^2$$

Equating this to thrust, T, where T is related to the power P, by

$$T = \frac{2P}{v} = \frac{2i \, Vapp}{\sqrt{\frac{2q}{m} V}} = \frac{3}{8} \theta^2 k^2 \epsilon_o V^2$$

we obtain,

$$i = \frac{3}{8\sqrt{2}} \sqrt{q/m} \quad \theta^2 k^2 \epsilon_o V^{\frac{3}{2}}$$

Note that this current is independent of the radius.

An alternate method of deriving this is instructive in understanding the phenomena of space charge limitation. We will picture the current as composed of sheets of charge equal to one half the surface charge on the tip of radius, r, over angle, θ, leaving the surface and accelerating to a distance of br when it no longer shields the tip from field and a new sheet starts out. The charge in such a sheet will be

$$q = \frac{1}{2} \theta^2 r^2 \epsilon_o E = \frac{1}{2} \theta^2 r \epsilon_o kV$$

The time τ to go a distance of br will be approximately

$$\tau = 2\frac{br}{v} = \frac{2br}{\sqrt{2\frac{q}{m} V}}$$

Then

$$i \simeq \frac{q}{\tau} \simeq \frac{\sqrt{2\frac{q}{m}}}{4} \theta^2 \frac{k}{b} \epsilon_o V^{\frac{3}{2}}$$

This equation is similar to the previous equation for i, is independent of r and would be the same if b is approximately $\frac{1}{k}$ or 5. We shall calculate this current for a charge to mass ratio,

$\frac{q}{m}$ = 400 coulombs/kg for V = 10,000 volts, for

$\Theta = \frac{1}{2}$ and k = .2

$$i = \frac{3}{8 \times 1.414} \times \sqrt{400} \times \frac{1}{4} .04 \times 8.85 \times 10^{-12} \times 10^{6}$$

$$\cong .45\mu a$$

This is about the value from a single needle. It would vary as the charge to mass varies and could be affected by the geometry which alters k and by the value Θ. In a sense this current is the total that can come from one or more jets from one needle or from an array of needles with a single distant accelerating electrode if the jets merge before the accelerating electrode is seen. The conclusion is that an array must have individual accelerating electrodes for each needle.

We can further develop the picture of the drop formation by developing a few simple relationships involving a single jet of 1/2 micro-amperes with a charge to mass ratio of 400 coulombs/kg at 10 KV. The mass flow would be

$$1/2 \times 10^{-6}/400 = 1.25 \times 10^{-9} \text{ kg/sec.}$$

There are large fields existing at the tip accelerating the liquid in the jet before the jet breaks up into droplets and so it is reasonable to assume the velocity of the jet at the time of break-up is 1/10 the final velocity v_f. Let us see what radius of jet going this velocity will deliver the mass flow.

$$M = \rho \times \text{Area} \times v = 1260 \times \pi r^2 \times 1/10 \sqrt{2 \times 400 \times 10^4} =$$

$$1.25 \times 10^{-9} \text{ kg/sec.}$$

then

$$r \cong 3.4 \times 10^{-8} \text{ meters} = 340 \text{ angstroms}$$

We might expect, then, a stream of about 700 angstroms in diameter breaking up into drops of that diameter.

The charge-to-mass ratio will allow us to derive the size of the droplets if we can deduce a reasonable criterion for the surface electric field. A limiting field strength might be set by the tensile strength of the material which would be about the value we will find but we choose to accept a relationship involving radius and surface tension. This Rayleigh relationship will indicate that larger droplets would be unstable under fields much smaller than the limiting field strength and would break up into smaller droplets at higher fields. This relationship, neglecting inertial effects and redistribution of charge as the drop distorts can be approximated by setting

$$\frac{\pi r^2 \epsilon_o E^2}{2} = 2\pi r \gamma$$

where γ is surface tension.

then

$$E = 2\sqrt{\frac{\gamma}{\epsilon_o r}}$$

Combining this with the relationship

$$\frac{q}{m} = \frac{q_s \text{ Area}}{\rho \text{ volume}} = \frac{\epsilon_o E \times 4\pi r^2}{\rho \frac{4}{3} \pi r^3} = \frac{3 \epsilon_o E}{\rho r}$$

we have,

$$r = \left[\frac{36\epsilon_o \gamma}{\rho^2 (q/m)^2} \right]^{1/3}$$

Taking

$$\gamma = 2.5 \times 10^{-2} \ \frac{\text{joules}}{\text{m}^2} \quad \text{for } \frac{q}{m} = 400$$

$$r = 3.2 \times 10^{-8} \text{ meters or 320 angstroms}$$

From this probable size of the droplet, we can further our picture. The mass, M, of the particles is:

$$M = \rho \frac{4}{3} \pi r^3 = 2 \times 10^{-19} \text{ kg}$$

A mass flow of 1.25×10^{-9}kg represents about 6.5×10^9 particles/sec at 10 KV, with a final velocity of 2.83 KM/sec. So for 1 cm distance the transit time is about 3.5 μ_s and there will be 2.3×10^4 particles in transit at any one time. If in a line the separation of particles will be 0.4 microns. From our model of the merged droplets at 1/10 this velocity, this spacing should be approximately 10 diameters.

It is very probable that the space charge of one droplet will cause the next droplet to be formed in a different direction so as to slightly spread the jet. It is observed however that a single jet is restricted to less than 5 degrees.

Conjecture as to any other aspects of the droplet formation is vague. Electrical acceleration couples with surface tension, inertial and viscous effects to produce the jet. When finally the inertial effects get so small that surface

tension can produce instability and form a drop, then the drops form. The resonant frequency of these drops is approximately

$$f \cong \frac{1}{2\pi} \sqrt{\frac{3\gamma}{r^3 \rho}} \cong 200 \text{ megacycles.}$$

This is near the formation rate of 6.5×10^9 sec and would indicate that about 10 particles are in different stages of separation at one time.

With a measured resistivity of 2000 Ω-cm, for 3% of antimony trichloride doped glycerol, the voltage drop per unit length at the tip of the jet is

$$\frac{i \times R}{\pi r^2} = \frac{1}{2} \frac{10^{-6} \times 2000}{\pi \times 3.3^2 \times 10^{-12}} \cong 3 \times 10^7 \frac{V}{cm}$$

This is comparable to the field necessary to induce the average field of about 10^7 V/cm on the particle.

This field on the particle is that established by the Rayleigh criterion. The potential $\phi = rE$ is 300 volts. These potentials and fields are consistent with assumption of acceleration to 1/10 of final velocity or more while still in the jet.

The potential of the particle is a measure of the energy of creation and not available for producing thrust. If accelerated through 1 million volts, the velocity of the droplet will be the same as if accelerated through 300 volts less. This point hardly effects the overall power efficiency.

Aeronautical Research Laboratories, Wright-Patterson AFB, O. RESEARCH ON THE GENERATION AND ACCELERATION OF SUBMICRON-SIZE PARTICLES by E. Cohen, Space Technology Labs., Inc., Redondo, Beach Calif. May 1963. 87 p. incl. illus. (Project 7116;Task 7116-03) (Contract AF 33(616)-6775) (ARL 63-88) Unclassified Report

The research involved in generating submicron-size positively charged liquid droplets is described. The droplets formed may be either liquid-metal, or organic fluids. An analysis is developed to indicate the relation-

(over)

UNCLASSIFIED

ship between particle size and the parameters of field emission and surface tension. Charge/mass ratios were obtained using either a single particle detector or one of two quadrupole focussing mass spectrometers. Charge/mass distributions are shown for both metals and organic fluids.

UNCLASSIFIED

Aeronautical Research Laboratories, Wright-Patterson AFB, O. RESEARCH ON THE GENERATION AND ACCELERATION OF SUBMICRON-SIZE PARTICLES by E. Cohen, Space Technology Labs., Inc., Redondo, Beach Calif. May 1963. 87 p. incl. illus. (Project 7116;Task 7116-03) (Contract AF 33(616)-6775) (ARL 63-88) Unclassified Report

The research involved in generating submicron-size positively charged liquid droplets is described. The droplets formed may be either liquid-metal, or organic fluids. An analysis is developed to indicate the relation-

(over)

UNCLASSIFIED

ship between particle size and the parameters of field emission and surface tension. Charge/mass ratios were obtained using either a single particle detector or one of two quadrupole focussing mass spectrometers. Charge/mass distributions are shown for both metals and organic fluids.

UNCLASSIFIED